

PROBABILITY OF PHYSICAL ASSOCIATION OF 104 BLENDED COMPANIONS TO *KEPLER* OBJECTS OF INTEREST USING VISIBLE AND NEAR-INFRARED ADAPTIVE OPTICS PHOTOMETRYDANI ATKINSON¹, CHRISTOPH BARANEC¹, CARL ZIEGLER², NICHOLAS LAW², REED RIDDLE³, AND TIM MORTON⁴*Draft version May 26, 2022*

ABSTRACT

We determine probabilities of physical association for stars in blended Kepler Objects of Interest, and find that $14.5^{+3.8}_{-3.4}\%$ of companions within $\sim 4''$ are consistent with being physically unassociated with their primary. This produces a better understanding of potential false positives in the Kepler catalog and will guide models of planet formation in binary systems. Physical association is determined through two methods of calculating multi-band photometric parallax using visible and near-infrared adaptive optics observation of 84 KOI systems with 104 contaminating companions within $\sim 4''$. We find no evidence that KOI companions with separation of less than $1''$ are more likely to be physically associated than KOI companions generally. We also reinterpret transit depths for 94 planet candidates, and calculate that $2.6\% \pm 0.4\%$ of transits have $R > 15R_{\oplus}$, which is consistent with prior modeling work.

Subject headings: binaries:close – planetary systems – planets and satellites: detection – planets and satellites: fundamental parameters

1. INTRODUCTION

The *Kepler* mission had a simple observing strategy: it observed a 105 deg^2 field in Cygnus near-continuously with an unfiltered wideband camera. Its main data output were the light curves of target stars, in which it found transits and measured their depth and timing. The conversion of this transit information to planetary characteristics requires the stellar parameters of the host, which the *Kepler* telescope could not provide itself. Stellar characterization is then dependent on data from other sources, typically photometric observations performed for the Kepler Input Catalog in the visible and by 2MASS in the near-infrared (Brown et al. 2011; Liebert et al. 1995; Huber et al. 2014).

A complication arises from the vulnerability of *Kepler*'s relatively large $4''$ pixels to the misinterpretation of unresolved binaries as single stars (Borucki et al. 2010). These unseen companions dilute the transit by making it appear shallower relative to its host star, and thus the transiting object's size is underestimated. Photometric characterization of the host star is also distorted by the blended light.

Many of these blended and contaminating companions can be identified in the *Kepler* data by careful examination of the light curve data for irregularities, including secondary transits (indicative of an eclipsing binary) and shifts in the star's centroid coincident with observed transits (Batalha et al. 2010; Tenenbaum et al. 2013). These techniques have proven largely successful in screening out many false positives, and though it has been shown that

of the remaining contaminated KOIs the great majority ($> 90\%$) are not false positives, many transiting planets are still larger than interpreted (Morton and Johnson 2011; Fressin et al. 2013; Santerne et al. 2013; Ciardi et al. 2015; Désert et al. 2015). Further validation then requires finding contaminating companions either indirectly, e.g. with transit photometry (Colón et al. 2012, 2015) or directly, e.g. high angular resolution imaging (Morton 2012). The necessary sub-arcsecond resolution to find these contaminating companions can be achieved on the ground by several techniques, most notably lucky/speckle imaging (Horch et al. 2012; Lillo-Box et al. 2012, 2014) and adaptive optics (Adams et al. 2012, 2013; Dressing et al. 2014).

With 6395 Kepler Objects of Interest (KOI) to vet (Coughlin et al. 2015), we adopted a strategy to conduct a comprehensive survey with Palomar 1.5-m/Robo-AO (Baranec et al. 2014, 2013) and use Keck II/NIRC2 to follow up on secure and likely detections of companions. To date we have reported the optical detection of 53 contaminating companions within $2.5''$ in a sample of 715 KOIs (Law et al. 2014) and 206 companions within $\sim 4''$ to 1629 KOIs (Baranec et al. 2016; Ziegler et al. 2016). The addition of near-infrared observations to the existing visible data permits us to perform characterization of the detected stars, estimate their photometric parallax and the likelihood of physical association between primary/companion pairs, and calculate reinterpreted sizes for individual planet candidates. In several cases we have also found additional unseen companions.

Section 2 of this paper describes the observations made and the image reduction process for Keck II/NIRC2 data. Section 3 describes the derivation of photometric and stellar characteristics from the objects studied, including techniques used for fitting to stellar type and results thereof. Section 4 discusses the spectral fit results in context of the entire KOI catalog. The paper concludes in Section 5 with an overview of our findings and an outline of future avenues of investigation.

Please direct correspondence to atkinson@ifa.hawaii.edu

¹ Institute for Astronomy, University of Hawai'i at Mānoa, Hilo, Hawai'i 96720-2700, USA² Division of Physics and Astronomy, University of North Carolina at Chapel Hill, Chapel Hill, NC 27599-3255, USA³ Division of Physics, Mathematics, and Astronomy, California Institute of Technology, Pasadena, CA 91125, USA⁴ Department of Astrophysical Sciences, Princeton University, Princeton, NJ 08544, USA

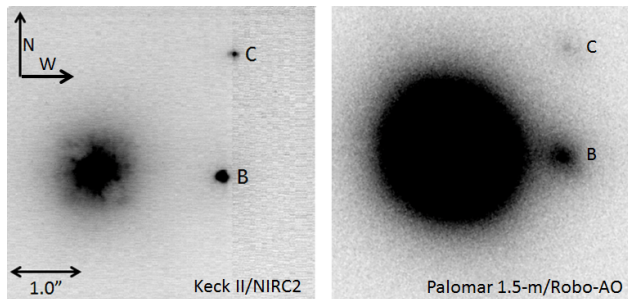


FIG. 1.— Images of KOI-268 from both Keck II/NIRC2 (left) and Palomar 1.5-m/Robo-AO, presented as an example. Visible in both images are companions B and C at separations from A of $1''.75$ and $2''.53$, respectively.

2. OBSERVATIONS AND DATA REDUCTION

The initial observations identifying companion candidates are from multiple Robo-AO observing runs on the Palomar Observatory 1.5-m telescope, spanning July to September 2012, April to October 2013, June to September 2014, and June 2015. Observations were in either Sloan-*i* or a long-pass 600nm (LP600) filter, the latter being similar to the *Kepler*-bandpass when combined with the EMCCD’s quantum efficiency curve for red/cool stars. Images were automatically reduced by the Robo-AO observing pipeline (Law et al. 2014).

The near-infrared observations are from the NIRC2 instrument on the 10-m Keck II telescope, conducted 2013 June 24, August 24 and 25, 2014 August 17, 2015 July 25, and August 4 in the *J*, *H*, *K*, and/or K_p filters in the narrow mode of NIRC2 ($9.952 \text{ mas pixel}^{-1}$; Yelda et al. 2010). For KOIs brighter than $m_V \sim 13$ we typically used the KOI as the guide star in natural guide star mode, and for fainter KOIs we used the laser guide star, with the KOI as the tip-tilt-focus guide star (Wizinowich et al. 2006; van Dam et al. 2006). An initial 30s exposure was taken for each target, and we waited for the low-bandwidth wavefront sensor to settle if the laser was used. The integration time and number of coadds per detector readout were adjusted to keep the peak of the stellar PSF counts less than 8,000 ADU per single integration (roughly half the dynamic range where sensitivity of the detector is linear), while maintaining a total exposure time of 30s. Dithered images were then acquired with the primary centered in the 3 lowest noise quadrants using the ‘bxy3 2.5’ command, for a total exposure time of 90s. Occasional dither failures, particularly on 4 Aug 2015, resulted in exposures where the target is centered on the detector.

Images are first sky-subtracted and then flat-fielded. A pipeline developed for this investigation is then used to automatically pick out companion stars by spatially binning pixels and selecting the locations of the brightest bins as candidates. These candidates then have their radius measured in the eight cardinal and intermediate directions from their local centroid. This measurement steps in the given direction until it finds a value consistent with the measured background value within a specified confidence interval (initially 3σ). If the median radius is both larger than a specified cutoff value (typically 3 pixels) and the standard deviation of the measured radii smaller than the same cutoff, the candidate is accepted as a star. The brightest star in the field

is assumed to be the primary unless manually specified otherwise (the narrow $10''$ NIRC2 field makes this a rare occurrence). If a companion is not found, the background confidence interval and radius cutoff are adjusted to optimize for close ($< 0''.5$) companions and the procedure repeated. If the procedure fails to find a companion, or if it finds multiple companions, a warning message notifies the operator to review the source image.

For the majority of targets the pipeline correctly locates the primary and any present companions, but manual validation is necessary for many targets largely because the speckles in the point spread function (PSF) are mistaken for stars. To avoid this misinterpretation the pipeline cross-references stars found in different filters for the same object, and discards any objects that do not appear in multiple filters. In some cases, images were only taken with one filter (typically K_p), and thus cross-referencing is not possible. These targets are then manually vetted and removed if visually confirmed to be associated with the primary PSF (i.e. coincident with rays projecting from the primary and presenting a PSF inconsistent with other imaged stars).

The separation and phase angle of each companion are measured from these individual reduced images, with uncertainties measured from the variability in measurements across all available images, and corrected for distortion using the most recent solution (Service et al. 2016). Last, images are co-added into a single composite image for each target and filter for use in photometry.

2.1. Aperture Photometry

For the majority of our Keck data, the diffraction-limited resolution makes simple aperture photometry sufficient for measuring the contrast between the two stars. To account for the overlap of the stars’ PSF envelopes, a matching aperture from the location opposite each star relative to its companion is used to estimate background subtraction, if available. In cases where the corresponding Robo-AO results were unavailable the method was also applied to those images, using the known position of the companion taken from the Keck analysis.

Systematic error from aperture size is our primary source of uncertainty, and is measured as the standard deviation of contrast across a range of aperture sizes from 1 to 3 FWHM in 0.5 FWHM increments. Injected companions are used to estimate further uncertainties typically yielding an error of 5%.

3. ANALYSIS

3.1. Photometric Classification of Stars

By combining our contrast measurements with extant *JHK* photometry for the blended system (from the Exoplanet Archive⁵) we derive the multi-color photometry for all components of each system. For blended magnitudes lacking a reported uncertainty (*i, Kep*), one was estimated based on the measurement’s reported source as recommended by the guide supplied by MAST (STScI 1997).⁶

⁵ <http://exoplanetarchive.ipac.caltech.edu> Most *JHK* magnitudes are from the 2MASS catalog (Liebert et al. 1995).

⁶ The documentation on *Kepler* magnitude sources at archive.stsci.edu/kepler/help/columns.html under heading ‘Kep-

Multi-color photometry allows characterization of the stars, necessary as the existing data on these objects is drawn from a blended target. Effective temperature is relatively strongly correlated with color-color photometry, but stellar radius (upon which our measurement of a transiting planet’s size is dependent) exhibits a much weaker correlation for late-type stars. To demonstrate the systematic biases inherent in photometric type-fitting, we present fitting results from 2 different photometric datasets.

The first dataset is a set of metallicity- and age-agnostic stellar SEDs, originally assembled from a heterogeneous set of models and data for an investigation of the Praesepe and Coma Berenices open clusters by Kraus and Hillenbrand (2007), henceforth KH07, and which has previously been used for photometric fitting of exoplanet host stars (e.g. Bechter et al. 2014; Wang et al. 2014, 2015). Photometric values for the *Kepler*-band were computed by the method described in Brown et al. (2011) using an arithmetic combination of *gri* colors. The list of types and magnitudes from KH07 is expanded with missing types linearly interpolated from existing data, and an additional 9 intermediate types also interpolated between each two adjacent integer stellar types (e.g. type G2.5 is linearly halfway between G2 and G3). This makes a table of 521 entries from B8 to L0 to be fitted to as standards, and with matching absolute magnitudes and radii. The interpolated decimal types are not reported directly but those entries are used to refine radius/distance estimates. Radii for spectral types are drawn from Habets and Heintze (1981).

To fit types we use a Monte Carlo technique, generating a Gaussian distribution for each of the photometric combinations $J-K$, $H-K$, $i-K$, and $Ke-K$, if information in the respective filters is present. K was chosen as the baseline as it produces the most precise contrast measurements and occupies the longest wavelength. Extinction is corrected for during this fitting process, relying on the canonical A_V for each target in the *Kepler* catalog and adjusted for the various filters/bandpasses via the standard relations from Cardelli et al. (1989): $A_{Kep} = 0.896A_V$, $A_i = 0.321A_V$, $A_J = 0.158A_V$, $A_H = 0.100A_V$, $A_K = 0.060A_V$.

Each time beginning in the center of the list of standards, the Gaussian-generated photometry is compared to each canonical type’s set of magnitudes to measure the error for all available data, as

$$R_{f1-f2} = (m_{f1,*} - m_{f2,*}) - (M_{f1,std} - M_{f2,std}) \quad (1)$$

where $m_{f\#,*}$ and $M_{f\#,typ}$ are the star’s measured apparent magnitude and the standard’s absolute magnitude in filters $f1$ and $f2$. The quality of the fit against the given standard is then

$$R^2 = \sum_{J,H,i,Kep} \frac{R_{filter-K}^2}{w_{filter-K}^2} \quad (2)$$

where $w_{filter-K}$ is the weight of the respective filter combination as

$$w_{filter-K} = \sqrt{\sigma_{filter}^2 + \sigma_K^2} \quad (3)$$

mag Source’ describes the respective uncertainties for the *Kepler* magnitude sources.

Note that Equation 2 does not require normalization as the number of filters used is consistent for a given star. R^2 is also measured for comparisons to standards in both directions (earlier- and later-type), and moved if a lower R^2 is found in either. The process repeats until it finds a minimum R^2 . The type, radius, and absolute magnitudes are recorded and the next member of the Gaussian-generated list is fit to the standards in the same way. After fitting every entry on the list, the means of type, radius, and absolute magnitudes are taken as the fitted values, and the standard deviation of the latter two are their uncertainties.

The second set is the *Kepler* Input Catalog’s (KIC) primary standard stars as reported in Brown et al. (2011), henceforth B11. The advantage of this catalog is that these stars are in the *Kepler* field and therefore reasonably representative of stars in our sample. The subset of standard stars with which each studied KOI component’s photometry is consistent to 1σ was used to compute a mean and standard deviation for the star’s stellar parameters. Subsets are typically 10% of the full list of primary standard stars (or ~ 30 stars) for each fitted object. Given the relatively poor correlation in the KIC standards of any of the measured stellar characteristics with NIR-only color comparisons, only $Ke-K$ and $i-K$ measurements were used. For stars without available Ke - or i -band measurements (with LP600 approximating Ke), a fit is not produced. If the photometry for a target fits two or fewer primary standard stars, its results are omitted. The effective temperature is then fit to a modeled stellar catalog to produce absolute magnitudes (Pecaut and Mamajek 2013), and compared to apparent magnitudes in turn to estimate distance. The KIC standard magnitudes were corrected for extinction/reddening as calculated from Schlafly and Finkbeiner (2011).

The fitted values for both methods are displayed in Table 1. The two methods are in broad agreement, although disparities are apparent for M-type companions in particular as the KIC primary standards contain few objects in that temperature range and exhibit a systemic overestimation of late-K and M-type radii that is not corrected for here (Muirhead et al. 2012). While the range of potential fit types for KH07 covered the full main sequence from B8 to M9, almost all stars fit to late types F-M.

Notably, two stars are presented as type B8, and five are too poorly restrained to produce KH07 fits. For the former, B8 is the end of the fitting range, and indicates they are too blue (adjusted for reddening) to fit to our list of main sequence stars. These stars are then very distant O/B types, and at 2 of 159 total stars analyzed by KH07 make up $\sim 1\%$ of the sample. As we are unable to fit above B8 their properties are not well constrained, and we present radius and distance as lower limits.

KH07 fitting fails to fit five stars in the sample due to relatively poor photometric constraints in one or more observation bands.

3.2. Uncertainties of Fitted Characteristics

As described above, the photometric uncertainties arise largely from sampling the contrast for a range of photometric apertures and the inherent 5% error measured by injection tests. For the stellar type fitting to KH07, the full Monte Carlo fit measures the uncertainty

of derived characteristics. Gaussian distributions matching each apparent magnitude measurement and uncertainty thereof are grouped into sets, and each set has its type and other fitted characteristics calculated by the method described above. The measured uncertainty in the derived characteristics is then the standard deviation of the full set of measurements. Uncertainties from the B11 fits are simply the measured standard deviations of the respective parameters of 1σ consistent KIC standard

stars. Uncertainties may be underestimated due to the granularity of the data being fit.

B11 also reports that use of photometric fitting on *Kepler* primary standard stars results in uncertainties of approximately 200K for effective temperature and 0.2 dex for stellar radius without prior constraints on stellar age or metallicity. We take this to be generally applicable to all our photometric type-fitting, but it is not factored into the uncertainties reported in Table 1.

TABLE 1 Fitted Stellar Parameters

object	via Kraus and Hillenbrand (2007)				via Brown et al. (2011)			
	<i>SpT</i>	R/R_{Sun}	$dist(pc)$	$\sigma_{unassoc}$	T_{eff}	R/R_{Sun}	$dist(pc)$	$\sigma_{unassoc}$
0190A	G0	$1.18^{+0.04}_{-0.07}$	921^{+127}_{-109}		6041^{+116}_{-129}	$1.04^{+0.03}_{-0.03}$	1019^{+52}_{-93}	
0190B	K3	$0.93^{+0.03}_{-0.02}$	716^{+89}_{-65}	1.46	4904^{+345}_{-265}	$0.83^{+0.13}_{-0.07}$	779^{+122}_{-77}	1.56
0191A	G0	$1.07^{+0.05}_{-0.03}$	934^{+82}_{-69}		5855^{+109}_{-184}	$1.00^{+0.02}_{-0.03}$	1115^{+93}_{-115}	
0191B	F4	$1.01^{+0.14}_{-0.07}$	2804^{+1007}_{-492}	3.75	5110^{+378}_{-472}	$0.94^{+0.09}_{-0.12}$	2573^{+651}_{-386}	3.67
0268A	F3	$1.29^{+0.06}_{-0.06}$	258^{+33}_{-34}		6136^{+143}_{-111}	$1.04^{+0.04}_{-0.03}$	230^{+18}_{-12}	
0268B	K4	$0.85^{+0.04}_{-0.06}$	315^{+33}_{-33}	1.22	4807^{+423}_{-282}	$0.79^{+0.16}_{-0.06}$	392^{+81}_{-41}	3.62
0268C	K3	$0.95^{+0.31}_{-0.08}$	904^{+3016}_{-290}	2.21	4889^{+660}_{-352}	$0.82^{+0.28}_{-0.08}$	829^{+354}_{-133}	4.46
0401A	G4	$1.05^{+0.02}_{-0.02}$	589^{+31}_{-44}		5890^{+152}_{-206}	$1.01^{+0.02}_{-0.03}$	744^{+70}_{-96}	
0401B	K7	$0.79^{+0.05}_{-0.08}$	690^{+74}_{-78}	1.20	5000^{+970}_{-554}	$0.88^{+0.33}_{-0.17}$	1185^{+716}_{-315}	1.37
0425A	F4	$1.22^{+0.05}_{-0.04}$	1374^{+212}_{-138}		6088^{+113}_{-165}	$1.02^{+0.04}_{-0.03}$	1425^{+95}_{-115}	
0425B	F2	$1.20^{+0.06}_{-0.07}$	1947^{+343}_{-253}	1.74	6013^{+116}_{-137}	$1.03^{+0.03}_{-0.03}$	2024^{+122}_{-177}	2.98
0511A	F3	$1.25^{+0.02}_{-0.04}$	1067^{+118}_{-118}		6128^{+112}_{-112}	$1.04^{+0.03}_{-0.03}$	1061^{+59}_{-59}	
0511B	K4	$0.84^{+0.04}_{-0.07}$	995^{+109}_{-115}	0.45	4796^{+456}_{-303}	$0.79^{+0.18}_{-0.06}$	1280^{+290}_{-149}	1.42
0511C	K6	$0.62^{+0.13}_{-0.16}$	2345^{+491}_{-609}	2.08				
0628A	F5	$1.24^{+0.02}_{-0.02}$	876^{+40}_{-46}		6085^{+113}_{-192}	$1.04^{+0.04}_{-0.03}$	856^{+51}_{-104}	
0628B	K9	$0.64^{+0.08}_{-0.11}$	1070^{+140}_{-180}	1.05				
0628C	K1	$0.85^{+0.05}_{-0.07}$	2247^{+254}_{-286}	4.75	4744^{+533}_{-329}	$0.74^{+0.21}_{-0.07}$	2809^{+820}_{-385}	5.03
0687A	F6	$1.24^{+0.02}_{-0.04}$	837^{+56}_{-72}		6012^{+119}_{-158}	$1.02^{+0.04}_{-0.03}$	806^{+55}_{-76}	
0687B	K4	$0.89^{+0.05}_{-0.07}$	699^{+116}_{-83}	1.01	5486^{+417}_{-300}	$1.02^{+0.15}_{-0.07}$	1114^{+311}_{-176}	1.67
0688A	F4	$1.30^{+0.01}_{-0.01}$	1204^{+49}_{-54}		6158^{+86}_{-158}	$1.03^{+0.02}_{-0.02}$	1057^{+50}_{-87}	
0688B	K0	$0.99^{+0.07}_{-0.04}$	1166^{+239}_{-125}	0.16	5122^{+342}_{-242}	$0.87^{+0.09}_{-0.03}$	1174^{+249}_{-142}	0.78
0712A	F1	$1.26^{+0.17}_{-0.17}$	1100^{+221}_{-221}		6228^{+169}_{-169}	$1.07^{+0.03}_{-0.03}$	1045^{+76}_{-76}	
0712B	K1	$0.95^{+0.05}_{-0.03}$	637^{+82}_{-54}	1.96	5204^{+472}_{-318}	$0.89^{+0.16}_{-0.09}$	762^{+220}_{-118}	1.22
0931A	F3	$1.27^{+0.04}_{-0.04}$	1720^{+195}_{-186}		6140^{+74}_{-106}	$1.05^{+0.03}_{-0.04}$	1654^{+57}_{-94}	
0931B					5943^{+139}_{-225}	$1.01^{+0.04}_{-0.03}$	6491^{+602}_{-817}	5.91
0984A	G5	$1.03^{+0.03}_{-0.02}$	267^{+21}_{-19}		5806^{+191}_{-270}	$1.00^{+0.05}_{-0.06}$	326^{+48}_{-44}	
0984B	G5	$1.03^{+0.03}_{-0.02}$	273^{+22}_{-19}	0.21	5717^{+302}_{-302}	$0.99^{+0.07}_{-0.07}$	317^{+46}_{-46}	0.14
0987A	G7	$1.01^{+0.01}_{-0.01}$	270^{+13}_{-6}		5656^{+241}_{-333}	$0.99^{+0.08}_{-0.08}$	325^{+55}_{-49}	
0987B	M0	$0.74^{+0.05}_{-0.05}$	458^{+47}_{-37}	4.79				
1066A	F6	$1.13^{+0.05}_{-0.05}$	1342^{+152}_{-108}		5932^{+102}_{-157}	$1.02^{+0.02}_{-0.03}$	1535^{+110}_{-145}	
1066B	G9	$0.85^{+0.03}_{-0.04}$	2894^{+245}_{-259}	5.17	4608^{+256}_{-285}	$0.74^{+0.06}_{-0.03}$	3333^{+289}_{-419}	4.15
1067A	F3	$1.29^{+0.01}_{-0.01}$	1431^{+60}_{-65}		6146^{+80}_{-205}	$1.04^{+0.03}_{-0.03}$	1280^{+72}_{-125}	
1067B	K2	$0.89^{+0.03}_{-0.02}$	2103^{+214}_{-175}	3.63	4833^{+409}_{-282}	$0.80^{+0.15}_{-0.06}$	2520^{+493}_{-269}	4.45
1112A	F5	$1.22^{+0.04}_{-0.06}$	1140^{+141}_{-160}		6160^{+88}_{-87}	$1.07^{+0.04}_{-0.03}$	1232^{+63}_{-43}	
1112B	K8	$0.73^{+0.04}_{-0.04}$	1528^{+120}_{-104}	2.21				
1151A	F9	$1.10^{+0.08}_{-0.05}$	501^{+76}_{-44}		5776^{+148}_{-270}	$0.99^{+0.02}_{-0.20}$	534^{+61}_{-71}	
1151B	K8	$0.71^{+0.19}_{-0.30}$	738^{+373}_{-289}	0.79	4620^{+488}_{-418}	$0.72^{+0.20}_{-0.07}$	991^{+240}_{-177}	2.44
1214A	G8	$1.00^{+0.02}_{-0.02}$	656^{+47}_{-26}		5600^{+256}_{-230}	$0.99^{+0.08}_{-0.07}$	836^{+136}_{-102}	
1214B	B8	≥ 1.5	≥ 5591	7.29				
1274A	G7	$1.00^{+0.01}_{-0.01}$	363^{+14}_{-9}		5602^{+250}_{-319}	$0.97^{+0.09}_{-0.08}$	443^{+76}_{-65}	
1274B	K9	$0.63^{+0.17}_{-0.26}$	585^{+191}_{-254}	0.87				
1375A	F5	$1.25^{+0.01}_{-0.02}$	809^{+28}_{-41}		6136^{+89}_{-103}	$1.05^{+0.04}_{-0.03}$	811^{+31}_{-47}	
1375B	K3	$0.88^{+0.21}_{-0.19}$	1862^{+1419}_{-480}	2.19	5097^{+433}_{-375}	$0.86^{+0.16}_{-0.09}$	2305^{+609}_{-325}	4.58
1442A	G4	$1.08^{+0.05}_{-0.03}$	322^{+26}_{-14}		5791^{+137}_{-294}	$0.99^{+0.02}_{-0.06}$	352^{+40}_{-50}	
1442B	M7	$0.30^{+0.16}_{-0.01}$	350^{+65}_{-29}	0.72				
1447A	A6	$1.45^{+0.04}_{-0.03}$	1206^{+62}_{-54}					
1447B	K3	$0.91^{+0.03}_{-0.02}$	517^{+43}_{-34}	9.98	4852^{+430}_{-216}	$0.77^{+0.17}_{-0.06}$	595^{+122}_{-59}	
1536A	F5	$1.27^{+0.01}_{-0.01}$	550^{+20}_{-18}		6229^{+71}_{-89}	$1.08^{+0.03}_{-0.03}$	551^{+19}_{-25}	
1536B	K3	$0.80^{+0.24}_{-0.34}$	1614^{+1388}_{-600}	1.77	5117^{+449}_{-439}	$0.87^{+0.15}_{-0.10}$	2169^{+607}_{-349}	4.63

TABLE 1 (continued)

object	via Kraus and Hillenbrand (2007)				via Brown et al. (2011)			
	SpT	$R(R_{Sun})$	$dist(pc)$	$\sigma_{unassoc}$	T_{eff}	$R(R_{Sun})$	$dist(pc)$	$\sigma_{unassoc}$
1546A	F2	$1.22^{+0.05}_{-0.09}$	1259^{+177}_{-256}		6116^{+75}_{-124}	$1.05^{+0.03}_{-0.03}$	1319^{+55}_{-80}	
1546B	K0	$0.93^{+0.06}_{-0.04}$	939^{+155}_{-98}	1.07	5111^{+384}_{-300}	$0.87^{+0.12}_{-0.10}$	1108^{+264}_{-148}	0.76
1546C					5873^{+429}_{-397}	$1.00^{+0.06}_{-0.10}$	5685^{+1077}_{-1181}	3.69
1546D	F7	$0.91^{+0.10}_{-0.08}$	2527^{+798}_{-415}	2.81	5208^{+386}_{-492}	$0.92^{+0.09}_{-0.12}$	3175^{+834}_{-522}	3.54
1613A	F5	$1.27^{+0.05}_{-0.05}$	404^{+60}_{-46}					
1613B	G4	$1.07^{+0.11}_{-0.09}$	419^{+101}_{-89}	0.14				
1700A	G8	$0.97^{+0.02}_{-0.02}$	602^{+36}_{-33}		5228^{+216}_{-261}	$0.89^{+0.06}_{-0.07}$	648^{+80}_{-68}	
1700B	K3	$0.89^{+0.03}_{-0.03}$	632^{+40}_{-40}	0.56	4614^{+409}_{-272}	$0.74^{+0.15}_{-0.06}$	685^{+119}_{-75}	0.34
1784A	F7	$1.16^{+0.05}_{-0.06}$	751^{+76}_{-73}		5939^{+100}_{-135}	$1.01^{+0.03}_{-0.03}$	817^{+54}_{-74}	
1784B	F2	$1.26^{+0.03}_{-0.06}$	1365^{+146}_{-176}	3.20	6113^{+85}_{-105}	$1.04^{+0.03}_{-0.03}$	1292^{+51}_{-68}	5.47
1845A	K2	$0.94^{+0.02}_{-0.01}$	411^{+24}_{-18}					
1845B	M4	$0.46^{+0.29}_{-0.19}$	651^{+445}_{-285}	0.84				
1845C	A7	$1.07^{+0.17}_{-0.10}$	4407^{+2110}_{-1089}	3.67				
1880A	K8	$0.78^{+0.01}_{-0.06}$	206^{+3}_{-17}					
1880B	G7	$0.93^{+0.07}_{-0.06}$	2094^{+492}_{-290}	6.51	4717^{+418}_{-334}	$0.76^{+0.16}_{-0.08}$	2046^{+365}_{-279}	
1884A	F9	$1.06^{+0.07}_{-0.04}$	1094^{+147}_{-123}		5890^{+159}_{-252}	$1.01^{+0.04}_{-0.05}$	1366^{+143}_{-193}	
1884B	K8	$0.63^{+0.17}_{-0.22}$	1381^{+449}_{-514}	0.54				
1884C	M1	$0.51^{+0.21}_{-0.15}$	1330^{+587}_{-424}	0.53				
1884D	M2	$0.41^{+0.17}_{-0.10}$	1335^{+642}_{-392}	0.58				
1891A	K0	$0.95^{+0.01}_{-0.02}$	687^{+27}_{-46}		5417^{+248}_{-158}	$0.97^{+0.08}_{-0.06}$	872^{+118}_{-93}	
1891B					5802^{+284}_{-402}	$1.00^{+0.06}_{-0.09}$	8742^{+1733}_{-1568}	5.00
1916A	F2	$1.31^{+0.01}_{-0.03}$	1046^{+43}_{-36}					
1916B	K5	$0.89^{+0.03}_{-0.04}$	672^{+85}_{-59}	4.05	4556^{+266}_{-276}	$0.73^{+0.08}_{-0.03}$	685^{+65}_{-84}	
1979A	F5	$1.23^{+0.02}_{-0.07}$	568^{+27}_{-59}		6012^{+110}_{-199}	$1.02^{+0.04}_{-0.03}$	547^{+41}_{-59}	
1979B	K9	$0.69^{+0.13}_{-0.23}$	454^{+98}_{-154}	1.00	4398^{+340}_{-569}	$0.70^{+0.04}_{-0.06}$	565^{+119}_{-182}	0.10
1989A	F9	$1.14^{+0.04}_{-0.03}$	525^{+49}_{-23}		5948^{+99}_{-124}	$1.02^{+0.03}_{-0.03}$	600^{+48}_{-40}	
1989B	K2	$0.90^{+0.03}_{-0.04}$	1299^{+195}_{-156}	4.73	5179^{+376}_{-447}	$0.86^{+0.14}_{-0.10}$	1536^{+353}_{-243}	3.78
2001A	K1	$0.97^{+0.01}_{-0.01}$	266^{+6}_{-6}		5386^{+264}_{-271}	$0.93^{+0.09}_{-0.07}$	318^{+52}_{-40}	
2001B	G5	$0.93^{+0.05}_{-0.03}$	1761^{+278}_{-200}	7.47	5123^{+396}_{-351}	$0.90^{+0.13}_{-0.09}$	2092^{+498}_{-270}	6.45
2009A	F7	$1.18^{+0.03}_{-0.03}$	696^{+59}_{-47}		6066^{+101}_{-155}	$1.05^{+0.03}_{-0.03}$	797^{+41}_{-82}	
2009B	K4	$0.82^{+0.07}_{-0.17}$	1204^{+196}_{-264}	1.88	4878^{+692}_{-381}	$0.82^{+0.33}_{-0.09}$	1715^{+767}_{-298}	3.05
2059A	K2	$0.93^{+0.02}_{-0.01}$	246^{+18}_{-14}		5104^{+315}_{-202}	$0.91^{+0.11}_{-0.06}$	288^{+54}_{-26}	
2059B	K5	$0.85^{+0.02}_{-0.03}$	268^{+22}_{-23}	0.75	4568^{+233}_{-288}	$0.73^{+0.06}_{-0.04}$	295^{+26}_{-37}	0.11
2069A	F7	$1.21^{+0.02}_{-0.03}$	723^{+52}_{-54}		5947^{+103}_{-147}	$1.02^{+0.03}_{-0.03}$	713^{+62}_{-53}	
2069B	K8	$0.71^{+0.13}_{-0.26}$	1266^{+407}_{-397}	1.36	4912^{+404}_{-419}	$0.80^{+0.15}_{-0.10}$	1874^{+383}_{-275}	4.12
2083A	G1	$1.16^{+0.10}_{-0.04}$	658^{+199}_{-57}		5889^{+152}_{-211}	$1.01^{+0.03}_{-0.03}$	685^{+66}_{-88}	
2083B	F7	$1.09^{+0.18}_{-0.38}$	1467^{+601}_{-923}	0.86	5139^{+1022}_{-481}	$0.85^{+0.26}_{-0.10}$	1178^{+697}_{-319}	1.51
2117A	K5	$0.86^{+0.01}_{-0.01}$	609^{+21}_{-26}					
2117B	K3	$0.88^{+0.01}_{-0.01}$	818^{+31}_{-33}	5.34	4640^{+768}_{-333}	$0.75^{+0.48}_{-0.08}$	988^{+436}_{-178}	
2143A	G2	$1.07^{+0.03}_{-0.03}$	643^{+39}_{-36}		5757^{+133}_{-206}	$1.00^{+0.02}_{-0.03}$	717^{+72}_{-74}	
2143B	A0	$1.19^{+0.21}_{-0.14}$	4408^{+4189}_{-1290}	2.92	5778^{+257}_{-364}	$0.99^{+0.06}_{-0.08}$	3590^{+667}_{-559}	5.10
2159A	F5	$1.26^{+0.01}_{-0.02}$	745^{+30}_{-45}		6130^{+87}_{-112}	$1.06^{+0.04}_{-0.03}$	739^{+30}_{-44}	
2159B	M0	$0.65^{+0.24}_{-0.27}$	742^{+373}_{-326}	0.01	4398^{+340}_{-569}	$0.70^{+0.04}_{-0.06}$	961^{+193}_{-306}	0.72
2247A	K3	$0.90^{+0.01}_{-0.01}$	337^{+11}_{-20}		4954^{+1280}_{-222}	$0.79^{+0.48}_{-0.07}$	528^{+383}_{-143}	
2247B	M0	$0.53^{+0.11}_{-0.10}$	1116^{+234}_{-234}	3.33				
2289A	F3	$1.30^{+0.01}_{-0.01}$	842^{+23}_{-27}		6201^{+64}_{-137}	$1.06^{+0.02}_{-0.02}$	753^{+32}_{-42}	
2289B	K6	$0.80^{+0.05}_{-0.08}$	1094^{+130}_{-140}	1.78	4620^{+807}_{-349}	$0.72^{+0.35}_{-0.08}$	1540^{+715}_{-296}	2.64
2317A	F7	$1.17^{+0.03}_{-0.05}$	817^{+58}_{-64}		5969^{+106}_{-128}	$1.01^{+0.03}_{-0.03}$	904^{+64}_{-67}	
2317B	G7	$0.88^{+0.02}_{-0.03}$	2661^{+219}_{-195}	9.06	4650^{+459}_{-296}	$0.75^{+0.19}_{-0.06}$	3029^{+603}_{-392}	5.35
2363A	K0	$0.95^{+0.01}_{-0.01}$	448^{+17}_{-19}		5386^{+360}_{-179}	$0.95^{+0.14}_{-0.07}$	578^{+129}_{-69}	
2363B	K3	$0.65^{+0.40}_{-0.30}$	3298^{+5208}_{-1596}	1.79	4923^{+515}_{-384}	$0.83^{+0.21}_{-0.08}$	4826^{+1448}_{-708}	5.90
2377A	F9	$1.08^{+0.10}_{-0.09}$	890^{+194}_{-181}					
2377B	K1	$0.92^{+0.05}_{-0.06}$	831^{+141}_{-104}	0.26				
2377C	K2	$0.64^{+0.38}_{-0.34}$	2449^{+3109}_{-1566}	0.99				
2377D	K7	$0.50^{+0.34}_{-0.22}$	1767^{+1465}_{-883}	0.97				
2413A	G7	$0.98^{+0.04}_{-0.03}$	756^{+78}_{-53}		5500^{+269}_{-258}	$0.99^{+0.08}_{-0.07}$	935^{+155}_{-127}	
2413B	M2	$0.48^{+0.21}_{-0.14}$	324^{+136}_{-173}	2.96				
2443A	F5	$1.21^{+0.03}_{-0.04}$	838^{+101}_{-101}		6141^{+87}_{-88}	$1.05^{+0.04}_{-0.03}$	934^{+33}_{-50}	
2443B	K6	$0.70^{+0.12}_{-0.22}$	1659^{+361}_{-504}	1.61	4742^{+878}_{-576}	$0.81^{+0.33}_{-0.12}$	2790^{+1614}_{-744}	2.49

TABLE 1 (continued)

object	via Kraus and Hillenbrand (2007)				via Brown et al. (2011)			
	SpT	$R(R_{Sun})$	$dist(pc)$	$\sigma_{unassoc}$	T_{eff}	$R(R_{Sun})$	$dist(pc)$	$\sigma_{unassoc}$
2542A	M0	$0.65^{+0.04}_{-0.08}$	278^{+18}_{-28}					
2542B	M3	$0.38^{+0.07}_{-0.06}$	218^{+49}_{-45}	1.06				
2601A	F3	$1.28^{+0.03}_{-0.05}$	1133^{+103}_{-141}		6214^{+75}_{-124}	$1.06^{+0.03}_{-0.03}$	1086^{+46}_{-58}	
2601B	G2	$1.07^{+0.19}_{-0.11}$	1193^{+560}_{-299}	0.19	5708^{+286}_{-393}	$0.98^{+0.06}_{-0.09}$	1283^{+249}_{-234}	0.83
2601C	G7	$0.93^{+0.07}_{-0.04}$	2076^{+411}_{-212}	4.00	4846^{+406}_{-299}	$0.78^{+0.14}_{-0.09}$	2236^{+443}_{-250}	4.52
2601D					5214^{+374}_{-568}	$0.90^{+0.08}_{-0.13}$	6068^{+1393}_{-1159}	4.30
2657A	G0	$1.09^{+0.07}_{-0.05}$	504^{+61}_{-48}		5859^{+127}_{-213}	$1.00^{+0.02}_{-0.03}$	585^{+56}_{-67}	
2657B	G6	$1.01^{+0.05}_{-0.02}$	454^{+54}_{-32}	0.69	5688^{+249}_{-269}	$1.00^{+0.06}_{-0.07}$	566^{+92}_{-78}	0.17
2664A	K0	$0.94^{+0.01}_{-0.01}$	868^{+50}_{-43}		5134^{+359}_{-167}	$0.87^{+0.15}_{-0.06}$	1025^{+208}_{-101}	
2664B	F6	$1.01^{+0.03}_{-0.03}$	1708^{+198}_{-136}	5.80	5620^{+252}_{-255}	$0.98^{+0.06}_{-0.07}$	2112^{+340}_{-286}	3.07
2681A	F7	$1.04^{+0.04}_{-0.03}$	1469^{+160}_{-133}		5763^{+202}_{-287}	$0.98^{+0.06}_{-0.06}$	1774^{+251}_{-254}	
2681B	K3	$0.88^{+0.01}_{-0.02}$	1191^{+68}_{-62}	1.86	4650^{+523}_{-340}	$0.75^{+0.26}_{-0.06}$	1366^{+332}_{-210}	0.98
2705A	M3	$0.39^{+0.13}_{-0.07}$	77^{+28}_{-16}					
2705B	M5	$0.30^{+0.08}_{-0.01}$	186^{+36}_{-11}	3.62				
2711A	F2	$1.28^{+0.02}_{-0.03}$	1193^{+77}_{-93}		6059^{+61}_{-129}	$1.03^{+0.03}_{-0.03}$	1072^{+40}_{-94}	
2711B	F2	$1.27^{+0.02}_{-0.03}$	1241^{+94}_{-115}	0.35	6059^{+57}_{-132}	$1.03^{+0.03}_{-0.04}$	1131^{+42}_{-99}	0.55
2722A	F3	$1.29^{+0.01}_{-0.01}$	808^{+21}_{-20}		6188^{+86}_{-158}	$1.05^{+0.02}_{-0.02}$	732^{+41}_{-47}	
2722B	K8	$0.69^{+0.06}_{-0.09}$	1341^{+132}_{-167}	3.17				
2779A	F3	$1.27^{+0.03}_{-0.04}$	1573^{+163}_{-161}		6140^{+74}_{-106}	$1.05^{+0.03}_{-0.04}$	1502^{+52}_{-86}	
2779B	G8	$0.95^{+0.12}_{-0.06}$	1793^{+608}_{-260}	0.72	5111^{+384}_{-373}	$0.87^{+0.12}_{-0.09}$	1991^{+472}_{-263}	1.82
2813A	K3	$0.93^{+0.01}_{-0.01}$	310^{+14}_{-12}		5128^{+443}_{-224}	$0.88^{+0.20}_{-0.07}$	383^{+106}_{-47}	
2813B	F8	$1.25^{+0.05}_{-0.09}$	1466^{+215}_{-195}	4.36	6049^{+122}_{-159}	$1.03^{+0.04}_{-0.03}$	1363^{+81}_{-140}	5.58
2813C	M1	$0.57^{+0.23}_{-0.21}$	3541^{+1995}_{-1484}	2.18	4887^{+1083}_{-835}	$0.89^{+0.32}_{-0.22}$	7753^{+5561}_{-2760}	2.67
2837A	F0	$1.40^{+0.05}_{-0.04}$	1430^{+125}_{-105}					
2837B	F0	$1.38^{+0.07}_{-0.04}$	1527^{+192}_{-122}	0.56				
2859A	G8	$0.98^{+0.02}_{-0.01}$	432^{+18}_{-9}		5582^{+196}_{-256}	$0.95^{+0.06}_{-0.07}$	546^{+81}_{-63}	
2859B	A7	$1.05^{+0.16}_{-0.22}$	2142^{+822}_{-896}	1.91	6169^{+140}_{-137}	$1.05^{+0.05}_{-0.03}$	2914^{+224}_{-180}	12.00
2869A	F4	$1.28^{+0.01}_{-0.01}$	919^{+29}_{-36}		6154^{+58}_{-145}	$1.05^{+0.03}_{-0.03}$	840^{+31}_{-60}	
2869B	K4	$0.63^{+0.09}_{-0.10}$	3401^{+481}_{-559}	4.43				
2904A	F5	$1.27^{+0.01}_{-0.02}$	587^{+27}_{-28}		6116^{+63}_{-212}	$1.05^{+0.03}_{-0.04}$	537^{+26}_{-68}	
2904B	A1	$1.28^{+0.11}_{-0.26}$	1976^{+470}_{-552}	2.51				
2971A	F4	$1.29^{+0.01}_{-0.01}$	622^{+18}_{-22}		6188^{+86}_{-158}	$1.05^{+0.02}_{-0.02}$	569^{+32}_{-37}	
2971B	G2	$0.96^{+0.04}_{-0.06}$	1712^{+236}_{-331}	3.29	5720^{+216}_{-289}	$0.99^{+0.05}_{-0.07}$	2281^{+363}_{-310}	5.49
2971C	K7	$0.47^{+0.33}_{-0.34}$	2446^{+2884}_{-1060}	1.72	5605^{+373}_{-590}	$0.96^{+0.08}_{-0.14}$	6324^{+1639}_{-1411}	4.08
3020A	F3	$1.31^{+0.01}_{-0.01}$	956^{+31}_{-28}					
3020B	K9	$0.77^{+0.03}_{-0.05}$	526^{+34}_{-37}	9.76				
3020C	K3	$0.77^{+0.07}_{-0.14}$	3032^{+479}_{-508}	4.08				
3069A	F4	$1.20^{+0.01}_{-0.05}$	1227^{+508}_{-162}		6110^{+89}_{-83}	$1.04^{+0.04}_{-0.03}$	1402^{+51}_{-62}	
3069B	K2	$0.90^{+0.01}_{-0.02}$	1164^{+58}_{-60}	0.32	4876^{+173}_{-134}	$0.81^{+0.04}_{-0.04}$	1332^{+87}_{-55}	0.66
3106A	G5	$1.04^{+0.05}_{-0.03}$	1189^{+142}_{-110}		5855^{+202}_{-287}	$1.00^{+0.05}_{-0.06}$	1526^{+207}_{-228}	
3106B	A3	$1.29^{+0.05}_{-0.06}$	3533^{+582}_{-576}	3.95	6188^{+88}_{-109}	$1.05^{+0.04}_{-0.03}$	3253^{+155}_{-151}	6.74
3377A	G9	$0.94^{+0.01}_{-0.01}$	675^{+24}_{-38}		5110^{+350}_{-160}	$0.94^{+0.16}_{-0.05}$	784^{+158}_{-73}	
3377B	M7	$0.29^{+0.01}_{-0.01}$	271^{+15}_{-14}	9.89				
3377C	M2	$0.36^{+0.09}_{-0.07}$	1215^{+405}_{-296}	1.82				
3401A	G8	$1.01^{+0.03}_{-0.02}$	665^{+60}_{-41}		5526^{+252}_{-277}	$0.93^{+0.07}_{-0.07}$	769^{+122}_{-110}	
3401B	B8	≥ 1.40	≥ 3510	6.69				
4004A	F8	$1.14^{+0.04}_{-0.04}$	400^{+32}_{-24}		5972^{+102}_{-135}	$1.02^{+0.02}_{-0.02}$	456^{+32}_{-35}	
4004B	K8	$0.75^{+0.05}_{-0.05}$	524^{+48}_{-43}	2.31				
4209A	F3	$1.09^{+0.11}_{-0.07}$	1647^{+385}_{-264}		6021^{+119}_{-135}	$1.02^{+0.03}_{-0.03}$	2124^{+125}_{-191}	
4209B	K7	$0.83^{+0.22}_{-0.43}$	1859^{+6446}_{-929}	0.21	4887^{+1083}_{-835}	$0.89^{+0.32}_{-0.22}$	1814^{+1305}_{-654}	0.24
4292A	G4	$1.06^{+0.03}_{-0.02}$	360^{+17}_{-16}		5857^{+140}_{-213}	$1.00^{+0.03}_{-0.03}$	436^{+43}_{-52}	
4292B	M6	$0.29^{+0.05}_{-0.01}$	610^{+48}_{-38}	6.01				
4331A	F2	$1.34^{+0.20}_{-0.13}$	1177^{+499}_{-283}		6140^{+140}_{-119}	$1.04^{+0.04}_{-0.03}$	964^{+76}_{-51}	
4331B	F3	$1.28^{+0.15}_{-0.15}$	1109^{+404}_{-299}	0.14	6033^{+136}_{-134}	$1.03^{+0.03}_{-0.03}$	962^{+58}_{-90}	0.03
4407A	F8	$1.17^{+0.05}_{-0.05}$	242^{+29}_{-24}					
4407A	G2	$1.14^{+0.05}_{-0.05}$	230^{+29}_{-18}	0.32				
4407B	K5	$0.82^{+0.06}_{-0.28}$	278^{+36}_{-87}	0.39				
4407C								
4463A	K8	$0.79^{+0.01}_{-0.02}$	427^{+14}_{-14}					

TABLE 1 (continued)

object	via Kraus and Hillenbrand (2007)				via Brown et al. (2011)			
	SpT	$R(R_{Sun})$	$dist(pc)$	$\sigma_{unassoc}$	T_{eff}	$R(R_{Sun})$	$dist(pc)$	$\sigma_{unassoc}$
4463B	K5	$0.85^{+0.02}_{-0.02}$	543^{+25}_{-28}	3.71				
4634A	A8	$1.33^{+0.05}_{-0.02}$	1223^{+136}_{-74}					
4634B	K2	$0.92^{+0.09}_{-0.06}$	669^{+202}_{-84}	2.58	4670^{+403}_{-349}	$0.73^{+0.13}_{-0.09}$	668^{+116}_{-90}	
4768A	G4	$1.01^{+0.02}_{-0.02}$	1037^{+91}_{-77}		5696^{+250}_{-282}	$0.99^{+0.07}_{-0.08}$	1330^{+237}_{-182}	
4768B	K5	$0.73^{+0.09}_{-0.15}$	2014^{+578}_{-507}	1.90				
4822A	F6	$1.27^{+0.05}_{-0.03}$	769^{+109}_{-67}		6127^{+83}_{-84}	$1.03^{+0.03}_{-0.04}$	733^{+25}_{-35}	
4822B	K9	$0.60^{+0.18}_{-0.17}$	1665^{+537}_{-564}	1.56				
4871A	F4	$1.28^{+0.01}_{-0.01}$	724^{+18}_{-25}					
4871B	A5	$1.22^{+0.08}_{-0.11}$	2540^{+545}_{-546}	3.32	6030^{+133}_{-134}	$1.03^{+0.03}_{-0.03}$	2556^{+155}_{-236}	
5578A	G5	$1.11^{+0.05}_{-0.04}$	190^{+17}_{-10}		6005^{+114}_{-157}	$1.00^{+0.02}_{-0.03}$	233^{+16}_{-21}	
5578B	G5	$1.07^{+0.12}_{-0.07}$	383^{+99}_{-61}	3.05	5778^{+201}_{-296}	$0.99^{+0.05}_{-0.06}$	438^{+70}_{-58}	3.41
5762A	G6	$0.99^{+0.03}_{-0.03}$	1130^{+146}_{-89}		5551^{+255}_{-293}	$0.95^{+0.07}_{-0.08}$	1385^{+230}_{-199}	
5762B	F4	$1.08^{+0.12}_{-0.07}$	2042^{+556}_{-342}	2.45	5886^{+193}_{-303}	$1.02^{+0.05}_{-0.06}$	2431^{+314}_{-400}	2.27

TABLE 1 Stellar parameters as a result of two different fitting techniques. $\sigma_{unassoc}$ is the certainty (in standard deviations) that each companion is physically unassociated with its host due to their respective distances. The Kraus & Hillenbrand fit yields a stellar type and corresponding radius (Kraus and Hillenbrand 2007). Values are interpolated between the table items in the source for improved precision. The fit to the KIC primary standards from Brown yields effective temperature and stellar radius for all stars with sufficient photometry, as produced by comparison to stars with similar color-color measurements among the 279 entries in the KIC Primary Standard catalog (Brown et al. 2011). As noted, photometric type-fitting of *Kepler* targets has been found to have a limiting accuracy of $\pm 200K$ and $\sim 0.2dex$ respectively, which is largely a function of age/composition and is not taken into account here. For each primary/companion pair a distance measurement was produced from the measured apparent and fitted absolute magnitudes, and used to generate a confidence of non-association between the two objects.

3.3. On Potential Giants

Dwarf-giant eclipsing binaries were originally expected to be approximately 200 times more abundant than detected planet-star transits in the *Kepler* field (Brown 2003). The assembly of the *Kepler* Input Catalog made use of Bayesian techniques to exclude most of these giants (Brown et al. 2011). Remaining dwarf-giant eclipsing binaries are identified and screened by the *Kepler* analysis pipeline, particularly by the presence of secondary eclipses in light curves (Batalha et al. 2010; Tenenbaum et al. 2013). Although a dwarf-giant eclipsing binary with (or as) a contaminating companion should be a relatively rare arrangement, it is reasonable to expect that some might still fall out of a dataset as large as the KIC. It has been demonstrated spectroscopically that a number of late-type *Kepler* Input Catalog stars photometrically characterized as dwarfs are in fact giants, but also that an improved photometric cut exists as $K_p - J > 2$ and $K_p < 14$ that contains $96\% \pm 1\%$ giants (with the corresponding $K_p - J > 2$ and $K_p > 14$ containing only $7\% \pm 3\%$), allowing us to investigate our updated photometry for the possibility of giants hiding in blended KOIs (Mann et al. 2012). None of our observed stars meet this set of criteria, and thus all objects are likely dwarfs.

3.4. Probability of Physical Association

Table 1 lists the confidence for each host/companion pair to be physically unassociated, derived from the respective distances and uncertainties of both fitting methods. The noted uncertainties in photometrically fitting

temperature/radius ($\pm 200K$ and $0.2dex$, respectively) to individual stars reported in B11 are ignored for the distance estimates and physical association confidences as they are functions of stellar age and metallicity, which should be consistent across all members of a physically associated system. We treat all pairs with $\geq 5\sigma$ level of confidence to be inconsistent with a physically associated/gravitationally bound scenario. Note that pairs with $\leq 5\sigma$ are not necessarily associated/bound but are not inconsistent with such an interpretation. The KH07 method then identifies 13 physically unassociated companions, while the B11 method finds 10.

The two methods agree to 5σ on the unboundedness of only one companion, 2001B. Of the other 12 unbound candidates via KH07, 9 do not have B11 fits, and one (2317B) has a marginal B11 $\sigma_{unassoc} = 4.90$. Only two, 1989B and 2664B, are unbound by KH07 and disputed by B11, for which the methods agree on distances but have respective B11 $\sigma_{unassoc}$ of 3.63 and 2.91 due to larger uncertainties on the B11 results.

B11 also identifies 10 additional physically unassociated companions that do not qualify by the KH07 measurement, though two (628C and 2813B) are marginal. We note that uncertainties for the B11 method are systematically underestimated by the granular dataset, and many could not be fit due to that catalog's relative sparsity, particularly for late-type stars.

The B11 results are presented to check the reproducibility of the KH07 fitting method, but given the noted issues with the former the KH07 results are preferred, and are the focus of this work.

TABLE 2 Adjusted Transit Depth and Candidate Sizes

object	A		B		C		D	
	depth (mmag)	R_{\oplus}	depth (mmag)	R_{\oplus}	depth (mmag)	R_{\oplus}	depth (mmag)	R_{\oplus}
0190.01	16.61 ± 0.026	$15.99^{+0.54}_{-0.94}$	57.24 ± 0.092	$22.98^{+0.99}_{-0.49}$				
0191.01	18.58 ± 0.027	$15.2^{+0.71}_{-0.43}$	345.0 ± 0.502	$60.31^{+7.41}_{-4.56}$				
0191.02	0.840 ± 0.013	$3.24^{+0.15}_{-0.09}$	13.55 ± 0.223	$12.87^{+1.6}_{-0.99}$				

object	A		B		C		D	
	depth (mmag)	R_{\oplus}	depth (mmag)	R_{\oplus}	depth (mmag)	R_{\oplus}	depth (mmag)	R_{\oplus}
0191.03	0.232 ± 0.009	1.71 ^{+0.08} _{-0.05}	3.739 ± 0.147	6.78 ^{+0.86} _{-0.53}	N/A	≥ 100.3		
0191.04	0.725 ± 0.030	3.01 ^{+0.15} _{-0.09}	11.69 ± 0.494	11.96 ^{+1.53} _{-0.94}				
0268.01	0.546 ± 0.003	3.13 ^{+0.1} _{-0.12}	127.9 ± 0.918	30.54 ^{+1.46} _{-2.56}				
0401.01	2.449 ± 0.016	5.44 ^{+0.16} _{-0.1}	35.30 ± 0.238	15.21 ^{+0.98} _{-1.77}				
0401.02	1.868 ± 0.043	4.75 ^{+0.14} _{-0.09}	26.83 ± 0.618	13.29 ^{+0.87} _{-1.57}				
0401.03	0.405 ± 0.019	2.21 ^{+0.07} _{-0.04}	5.775 ± 0.282	6.19 ^{+0.42} _{-0.75}				
0425.01	23.09 ± 0.065	19.46 ^{+0.79} _{-0.63}	51.76 ± 0.147	28.23 ^{+1.42} _{-1.65}				
0511.01	0.757 ± 0.009	3.6 ^{+0.05} _{-0.15}	13.15 ± 0.173	10.05 ^{+0.48} _{-0.97}	278.9 ± 3.670	30.62 ^{+7.36} _{-7.88}		
0511.02	0.210 ± 0.008	1.9 ^{+0.05} _{-0.08}	3.645 ± 0.146	5.3 ^{+0.26} _{-0.52}	70.73 ± 2.846	16.16 ^{+3.98} _{-4.26}		
0688.01	0.354 ± 0.006	2.56 ^{+0.02} _{-0.04}	2.608 ± 0.048	5.39 ^{+0.43} _{-0.27}				
0984.01	2.187 ± 0.013	5.04 ^{+0.15} _{-0.1}	2.376 ± 0.014	5.25 ^{+0.15} _{-0.1}				
0987.01	0.232 ± 0.005	1.61 ^{+0.02} _{-0.02}	6.369 ± 0.139	6.42 ^{+0.26} _{-0.43}				
1066.01	15.39 ± 0.032	14.62 ^{+0.65} _{-0.65}	1261. ± 2.662	76.84 ^{+2.72} _{-3.62}				
1067.01	50.95 ± 0.069	30.12 ^{+0.23} _{-0.23}	N/A	≥ 93.78				
1112.01	0.689 ± 0.022	3.38 ^{+0.11} _{-0.17}	50.69 ± 1.648	17.0 ^{+1.2} _{-0.96}				
1214.01	0.294 ± 0.018	1.79 ^{+0.04} _{-0.04}	0.890 ± 0.056	5.0 ^{+0.3} _{-0.33}				
1447.01	228.6 ± 0.074	68.91 ^{+1.9} _{-1.43}	N/A	≥ 97.05				
1447.02	17.96 ± 0.038	20.25 ^{+0.56} _{-0.42}	125.5 ± 0.267	32.79 ^{+1.08} _{-0.72}				
1700.01	0.442 ± 0.016	2.13 ^{+0.05} _{-0.05}	1.174 ± 0.042	3.19 ^{+0.11} _{-0.11}				
1784.01	7.479 ± 0.092	10.48 ^{+0.46} _{-0.55}	12.74 ± 0.157	14.96 ^{+0.36} _{-0.6}				
1880.01	0.680 ± 0.009	2.13 ^{+0.03} _{-0.14}	18.33 ± 0.248	13.83 ^{+1.29} _{-0.71}	228.7 ± 3.558	27.57 ^{+11.09} _{-9.64}	356.4 ± 5.543	23.07 ^{+10.38} _{-5.77}
1884.01	3.201 ± 0.049	6.27 ^{+0.42} _{-0.24}	123.3 ± 1.919	26.09 ^{+5.08} _{-9.79}				
1884.02	0.618 ± 0.039	2.76 ^{+0.19} _{-0.11}	22.80 ± 1.459	11.47 ^{+2.33} _{-4.5}	40.66 ± 2.603	12.13 ^{+5.1} _{-4.44}	60.42 ± 3.868	10.15 ^{+4.84} _{-2.69}
1916.01	0.395 ± 0.009	2.73 ^{+0.02} _{-0.02}	4.866 ± 0.115	7.0 ^{+0.45} _{-0.37}				
1916.02	0.305 ± 0.006	2.39 ^{+0.02} _{-0.02}	3.754 ± 0.079	6.15 ^{+0.39} _{-0.33}				
1916.03	0.079 ± 0.004	1.22 ^{+0.01} _{-0.01}	0.980 ± 0.051	3.14 ^{+0.21} _{-0.17}				
1989.01	0.534 ± 0.020	2.76 ^{+0.1} _{-0.08}	13.31 ± 0.505	11.08 ^{+0.37} _{-0.37}				
2001.01	0.205 ± 0.007	1.45 ^{+0.02} _{-0.02}	13.88 ± 0.502	11.43 ^{+0.64} _{-0.38}				
2009.01	0.626 ± 0.022	3.06 ^{+0.08} _{-0.11}	25.22 ± 0.901	13.72 ^{+1.2} _{-3.59}				
2059.01	0.186 ± 0.007	1.33 ^{+0.03} _{-0.01}	0.509 ± 0.020	2.01 ^{+0.05} _{-0.07}				
2059.02	0.057 ± 0.005	0.74 ^{+0.02} _{-0.01}	0.156 ± 0.015	1.11 ^{+0.03} _{-0.04}				
2069.01	0.678 ± 0.013	3.3 ^{+0.06} _{-0.08}	29.60 ± 0.605	12.7 ^{+2.19} _{-4.92}				
2083.01	0.399 ± 0.015	2.49 ^{+0.17} _{-0.13}	1.027 ± 0.039	4.16 ^{+0.24} _{-1.01}				
2117.01	1.519 ± 0.074	3.51 ^{+0.04} _{-0.04}	2.060 ± 0.101	4.18 ^{+0.05} _{-0.05}				
2247.01	0.205 ± 0.011	1.35 ^{+0.02} _{-0.02}	20.34 ± 1.121	8.02 ^{+1.72} _{-1.72}				
2289.01	0.369 ± 0.018	2.61 ^{+0.02} _{-0.02}	28.81 ± 1.470	14.12 ^{+0.92} _{-1.48}				
2289.02	0.175 ± 0.009	1.8 ^{+0.01} _{-0.01}	13.57 ± 0.761	9.72 ^{+0.64} _{-1.02}				
2317.01	0.149 ± 0.009	1.5 ^{+0.04} _{-0.07}	16.21 ± 1.076	11.68 ^{+0.28} _{-0.42}				
2363.01	0.204 ± 0.012	1.42 ^{+0.02} _{-0.02}	45.44 ± 2.821	14.13 ^{+8.65} _{-6.78}				
2413.01	0.531 ± 0.029	2.39 ^{+0.15} _{-0.08}	3.329 ± 0.184	2.53 ^{+1.27} _{-0.89}				
2413.02	0.457 ± 0.038	2.22 ^{+0.14} _{-0.07}	2.868 ± 0.238	2.35 ^{+1.21} _{-0.85}				
2443.01	0.110 ± 0.007	1.33 ^{+0.04} _{-0.05}	13.41 ± 0.877	8.7 ^{+1.41} _{-2.82}				
2443.02	0.105 ± 0.008	1.3 ^{+0.03} _{-0.05}	12.79 ± 1.084	8.5 ^{+1.4} _{-2.81}				
2542.01	0.576 ± 0.033	1.63 ^{+0.13} _{-0.21}	1.710 ± 0.100	1.64 ^{+0.37} _{-0.27}				
2657.01	0.091 ± 0.007	1.09 ^{+0.08} _{-0.05}	0.117 ± 0.010	1.16 ^{+0.07} _{-0.04}				
2664.01	1.377 ± 0.105	3.65 ^{+0.04} _{-0.04}	2.954 ± 0.226	5.74 ^{+0.18} _{-0.12}				
2681.01	8.139 ± 0.129	9.8 ^{+0.38} _{-0.29}	26.00 ± 0.413	14.76 ^{+0.17} _{-0.34}				
2681.02	1.006 ± 0.111	3.45 ^{+0.15} _{-0.11}	3.193 ± 0.353	5.2 ^{+0.07} _{-0.13}				
2705.01	0.745 ± 0.027	1.31 ^{+0.53} _{-0.27}	11.40 ± 0.416	3.34 ^{+0.69} _{-0.12}				
2711.01	0.442 ± 0.013	2.82 ^{+0.05} _{-0.07}	0.493 ± 0.015	2.95 ^{+0.05} _{-0.1}				
2711.02	0.351 ± 0.016	2.51 ^{+0.04} _{-0.06}	0.392 ± 0.018	2.63 ^{+0.04} _{-0.09}				
2722.01	0.161 ± 0.004	1.72 ^{+0.01} _{-0.01}	60.00 ± 1.601	17.45 ^{+1.55} _{-2.33}				
2722.02	0.154 ± 0.005	1.68 ^{+0.01} _{-0.01}	57.25 ± 1.971	17.05 ^{+1.53} _{-2.3}				
2722.03	0.109 ± 0.003	1.41 ^{+0.01} _{-0.01}	40.34 ± 1.439	14.37 ^{+1.29} _{-1.94}				
2722.04	0.115 ± 0.005	1.45 ^{+0.01} _{-0.01}	42.41 ± 1.847	14.73 ^{+1.33} _{-2.0}				
2722.05	0.105 ± 0.006	1.39 ^{+0.01} _{-0.01}	38.80 ± 2.471	14.1 ^{+1.3} _{-1.95}				
2779.01	0.592 ± 0.028	3.23 ^{+0.08} _{-0.08}	6.113 ± 0.292	7.76 ^{+1.02} _{-0.51}				
2813.01	0.205 ± 0.017	1.4 ^{+0.02} _{-0.02}	0.506 ± 0.042	2.97 ^{+0.13} _{-0.23}	38.89 ± 3.261	11.66 ^{+4.86} _{-4.64}		
2837.01	0.259 ± 0.010	2.36 ^{+0.09} _{-0.07}	0.320 ± 0.013	2.59 ^{+0.14} _{-0.08}				
2849.01	0.205 ± 0.014	1.38 ^{+0.02} _{-0.03}	0.435 ± 0.029	4.54 ^{+0.65} _{-0.81}				
2859.01	0.100 ± 0.007	1.04 ^{+0.02} _{-0.01}	0.707 ± 0.054	2.53 ^{+0.42} _{-0.54}				

object	A		B		C		D	
	depth (mmag)	R_{\oplus}	depth (mmag)	R_{\oplus}	depth (mmag)	R_{\oplus}	depth (mmag)	R_{\oplus}
2859.02	0.068 ± 0.006	$0.86^{+0.02}_{-0.01}$	0.482 ± 0.044	$2.09^{+0.35}_{-0.45}$				
2859.03	0.078 ± 0.007	$0.92^{+0.02}_{-0.01}$	0.556 ± 0.053	$2.25^{+0.38}_{-0.48}$				
2859.04	0.077 ± 0.006	$0.91^{+0.02}_{-0.01}$	0.544 ± 0.044	$2.22^{+0.37}_{-0.47}$				
2859.05	0.107 ± 0.008	$1.07^{+0.02}_{-0.01}$	0.756 ± 0.062	$2.62^{+0.43}_{-0.56}$				
2869.01	0.139 ± 0.009	$1.58^{+0.01}_{-0.01}$	N/A	≥ 58.89				
2904.01	0.144 ± 0.005	$1.6^{+0.01}_{-0.03}$	0.895 ± 0.033	$3.6^{+0.45}_{-0.71}$				
2971.01	0.071 ± 0.004	$1.14^{+0.01}_{-0.01}$	2.705 ± 0.155	$5.28^{+0.23}_{-0.34}$	21.15 ± 1.214	$4.85^{+12.94}_{-0.8}$		
2971.02	0.103 ± 0.006	$1.37^{+0.01}_{-0.01}$	3.938 ± 0.260	$6.36^{+0.28}_{-0.42}$	30.91 ± 2.042	$5.85^{+15.73}_{-0.97}$		
3020.01	0.106 ± 0.006	$1.42^{+0.01}_{-0.01}$	2.122 ± 0.134	$3.71^{+0.15}_{-0.26}$	137.1 ± 8.661	$28.92^{+2.63}_{-4.88}$		
3069.01	0.387 ± 0.031	$2.47^{+0.09}_{-0.13}$	2.996 ± 0.244	$5.15^{+0.06}_{-0.12}$				
3377.01	0.476 ± 0.044	$2.15^{+0.02}_{-0.02}$	15.94 ± 1.488	$3.82^{+0.01}_{-0.01}$	100.9 ± 9.425	$11.37^{+2.92}_{-2.27}$		
3401.01	0.200 ± 0.022	$1.5^{+0.05}_{-0.03}$	0.452 ± 0.049	$3.32^{+0.25}_{-0.22}$				
3401.02	0.603 ± 0.061	$2.6^{+0.08}_{-0.06}$	1.362 ± 0.139	$5.75^{+0.42}_{-0.38}$				
4004.01	0.151 ± 0.010	$1.47^{+0.05}_{-0.05}$	6.263 ± 0.440	$6.2^{+0.44}_{-0.44}$				
4209.01	1.439 ± 0.350	$4.25^{+0.45}_{-0.4}$	13.51 ± 3.292	$13.95^{+2.43}_{-2.28}$				
4292.01	0.045 ± 0.004	$0.75^{+0.03}_{-0.02}$	50.35 ± 4.668	$6.73^{+1.52}_{-0.0}$				
4331.01	0.125 ± 0.011	$1.59^{+0.37}_{-0.19}$	0.157 ± 0.013	$1.72^{+0.38}_{-0.21}$				
4463.01	0.372 ± 0.024	$1.6^{+0.02}_{-0.06}$	0.376 ± 0.024	$1.7^{+0.04}_{-0.04}$				
4634.01	0.118 ± 0.012	$1.51^{+0.06}_{-0.03}$	0.618 ± 0.066	$2.39^{+0.29}_{-0.2}$				
4768.01	0.598 ± 0.062	$2.58^{+0.06}_{-0.06}$	24.00 ± 2.489	$11.77^{+1.77}_{-2.66}$				
4822.01	0.035 ± 0.003	$0.79^{+0.03}_{-0.02}$	19.46 ± 2.083	$8.57^{+2.89}_{-2.73}$				
4871.01	0.029 ± 0.004	$0.73^{+0.01}_{-0.01}$	0.524 ± 0.070	$2.87^{+0.22}_{-0.3}$				
4871.02	0.038 ± 0.004	$0.83^{+0.01}_{-0.01}$	0.671 ± 0.081	$3.25^{+0.24}_{-0.33}$				
5578.01	0.193 ± 0.025	$1.62^{+0.08}_{-0.07}$	0.997 ± 0.133	$3.54^{+0.49}_{-0.26}$				
5762.01	0.484 ± 0.065	$2.28^{+0.08}_{-0.08}$	0.876 ± 0.118	$3.35^{+0.42}_{-0.25}$				

TABLE 2 The transit depth and radius relative to potential host for all transit candidates, evaluated for association with all possible host stars. Evaluated only for KOIs with Kepler-band contrast observations. Candidates with radii lower limits indicate the depth of the eclipse is equal to or greater than the star’s full light.

3.5. Updated Transiting Object Parameters

For KOI systems observed in the *Kepler* band, we reinterpret the relative depth and size of all transit candidates in Table 2, relying on the KH07 results as new stellar characteristics. As we lack the ability to determine whether the primary or a companion is the host of the transiting object, all possible scenarios are presented. Note that these derivations require knowledge of each KOI component’s luminosity in the transit band, and thus only candidates with resolved LP600 photometry are shown. As mentioned in section 2, the LP600 combined with the EMCCD’s sensitivity curve approximates the *Kepler* passband, suppressing blue wavelengths that experience less benefit from adaptive optics correction.

With the new planet candidate sizes we estimate the probability each has a radius $R > 15R_{\oplus}$, the rough position of the boundary between gas giants and late-type stars. We then assume that every star in a blended KOI is an equally likely host for the transit, and measure an overall $P(R > 15R_{\oplus})$ as the mean average of probabilities for all possible hosts. This identifies potential false positives but does not constitute a full false positive calculation. Table 3 shows the results for all candidates for with $P(R > 15R_{\oplus}) \geq 0.01$. We did not take into account the relative prevalence of planetary bodies and brown dwarfs, which might indicate that planets are generally more likely system members and invalidate the assumption that all possible configurations are equally likely.

Three candidates have been identified elsewhere as false positives. Likely the largest transiting object, KOI1447.01 appears in the *Kepler* Eclipsing Binary Catalog (Slawson et al. 2011). KOI0190.01 has a disposition

of FALSE POSITIVE in the Exoplanet Archive from radial velocity measurements. KOI1112.01 has been identified as a false positive via ephemeris matching with the nearby KOI4720 by Coughlin et al. (2014), which notes that two stars are separated by only $4''.8$, and states that the transit host is believed to be a third then-unobserved object. This implies the host is KOI1112B, which elevates our estimate to $P(R > 15R_{\oplus}) = 0.95$.

4. DISCUSSION

Probabilities and uncertainties in this section are computed binomially by the method described in Burgasser et al. (2003).

Of the 93 companions with sufficient photometry, 13 (or $14.0\%^{+4.4\%}_{-2.9\%}$) are inconsistent with physical association with their primaries via KH07, while the B11 method gives 10 unassociated companions out of 53 examined (or $18.9\%^{+6.5\%}_{-4.2\%}$). All others are $< 5\sigma$ consistent with a bound interpretation. Simulations have previously demonstrated that the vast majority (96%) of narrowly-separated companions ($< 1.0''$) are physically associated (Horch et al. 2014). As 6 out of 40 (or $15\%^{+7.3\%}_{-4.0\%}$) narrowly-separated primary/companion pairs with fit results are inconsistent with a bound interpretation to 5σ , our results are inconsistent with the Horch prediction to $\sim 2.3\sigma$ and we see no evidence that narrowly separated ($< 1.0''$) companions are more likely to be physically associated than KOI companions in general or than widely-separated companions, for which we determine 7 of 53 or $13.2\%^{+6.0\%}_{-3.3\%}$ are unbound.

Via transit reinterpretation we have 38 potential non-

TABLE 3
PROBABILITY OF $R > 15R_{\oplus}$ FOR EACH PLANET CANDIDATE

KOI	P_A	P_B	P_C	P_D	P_{total}
0190.01 ^a	0.85	1.00			0.93
0191.01	0.68	1.00			0.84
0191.02	0	0.09			0.05
0191.04	0	0.02			0.01
0268.01	0	1.00	1.00		0.67
0401.01 ^b	0	0.55			0.27
0401.02 ^b	0	0.03			0.01
0425.01	1.00	1.00			1.00
0511.01 ^b	0	0	0.98		0.33
0511.02 ^b	0	0	0.61		0.20
1066.01	0.30	1.00			0.65
1067.01	1.00	1.00			1.00
1112.01 ^c	0	0.95			0.48
1447.01 ^c	1.00	1.00			1.00
1447.02	1.00	1.00			1.00
1784.01	0	0.46			0.23
1880.01	0	0.18			0.09
1884.01	0	0.87	0.90	0.92	0.65
1884.02	0	0.07	0.29	0.14	0.21
2009.01	0	0.14			0.07
2069.01	0	0.15			0.07
2289.01 ^b	0	0.17			0.09
2363.01	0	0.46			0.23
2681.01	0	0.08			0.04
2722.01 ^b	0	0.85			0.43
2722.02 ^b	0	0.81			0.41
2722.03 ^b	0	0.31			0.16
2722.04 ^b	0	0.42			0.21
2722.05	0	0.24			0.12
2813.01	0	0	0.25		0.08
2869.01	0	1.00			0.50
2971.01	0	0	0.22		0.07
2971.02	0	0	0.28		0.09
3020.01	0	0	1.00		0.33
3377.01	0	0	0.11		0.04
4209.01	0	0.33			0.16
4768.01	0	0.03			0.02
4822.01	0	0.01			0.01

^a Disposition is FALSE POSITIVE in the Exoplanet Archive as of 18 Sep 2015.

^b Disposition is CONFIRMED in the Exoplanet Archive as of 18 Sep 2015.

^c Other literature indicates candidate is false positive.

Estimated probabilities that each KOI planet candidate has a radius $R > 15R_{\oplus}$, for each potential host and summed across all. Only candidates for with $P(R > 15R_{\oplus}) \geq 0.01$ are listed. For full transit depth and planet size estimates, see Table 2.

planetary objects out of 88 reinterpreted transiting objects. By summing the computed $P(R > 15R_{\oplus})$ values this sample has a mean of $12.8^{+3.5}_{-3.1}$, or $14.5\%^{+4.0\%}_{-3.5\%}$ of candidates with $(R > 15R_{\oplus})$. Considered with the previously reported $17.6\% \pm 1.5\%$ nearby-star (companion) probability of Baranec et al. (2016), we estimate a $(R > 15R_{\oplus})$ rate due to unresolved companions to be $2.6\% \pm 0.4\%$. This is a rough measurement of false positives in the KOI catalog and is easily consistent with the broad $< 10\%$ false positive rate predicted by modeling (Morton and Johnson 2011).

On the whole, the derived planet candidate sizes are only slightly larger than estimates from Law et al. (2014), henceforth L14. The exceptions are primarily those candidates listed in Table 3. These are much larger than the L14 predictions as our analysis includes new sizes for the host stars and accounts for the change in distance estimates, whereas L14 used the original *Kepler* predictions derived from blended light.

4.1. KOI0191: Possible Coincident Multiple

L14 noted that this system is *a priori* unusual as the only multi-candidate KOI to have a large Jupiter-class candidate ($> 10R_{\oplus}$) in a very close orbit ($P < 20d$). Assuming binarity (of KOI0191A/B), L14 calculated a planetary candidate size of $11.3R_{\oplus}$ for the A scenario and $29.3R_{\oplus}$ for B, making the potential KOI0191B/KOI0191.01 system a close eclipsing binary in a hierarchical triple. With the inclusion of *JHK* photometry, we revise these estimates upward to $13.9R_{\oplus}$ and $55.9R_{\oplus}$, respectively.

Although hot Jupiters were previously thought inconsistent with other short-period planets, the discovery of multiple planets in the WASP-47 system proves the arrangement does exist in nature (Becker et al. 2015). Thus, we can not rule out that all four candidates are hosted by KOI0191A and are then planets.

4.2. KOI0268: No Longer Habitable

Both companions of KOI0268 have also been reported in Adams et al. (2012). KOI0268.01 was originally identified as a potentially habitable super-Earth with a radius of $1.7 R_{\oplus}$ and equilibrium temperature of 295 K. L14 reports both companions, and notes that if the planet orbits either of them rather than the target A, the equilibrium temperature of the planet will probably not be in the habitable range. The candidate's equilibrium temperature in literature has since been revised upward from 295K to 470K as reported in the Exoplanet Archive. Our fitted stellar types (from KH07) yield an uninhabitable surface temperature of 650K if hosted by A. For B and C both we estimate a surface temperature of $\sim 350K$, marginally allowing for the presence of liquid water, but the reinterpreted sizes imply a gas giant hosted by B or an eclipsing binary at C. Exomoons notwithstanding, this rules out habitability for KOI0268.01.

4.3. KOI1447: Double Eclipsing Binary

Both KOI1447.01 and KOI1447.02 are likely too large to be planets for either potential host, and .01 was included in the second release of the Kepler Eclipsing Binary Stars catalog (Slawson et al. 2011). Given the size of both candidates and their short orbital periods (40.2d and 2.3d, respectively), it seems likely they would conflict with each other if in the same system. KOI1447 is then a unique double false positive, consisting of two merely visually associated eclipsing binaries with coincidentally low inclination.

5. CONCLUSIONS

We have obtained visible and near-infrared multi-wavelength photometry of 104 blended companions to 84 KOIs, validating the original detections by Robo-AO. We report additional companions not originally detected by Robo-AO's original investigation. We find that $14.5\%^{+3.8\%}_{-3.4\%}$ of the investigated companions are physically unassociated with their KOI primaries at the 5σ level. Additional follow-up is recommended to confirm this result, with spectroscopy of both targets the best means of measuring $\log g$ to confirm actual sizes and distances, and to provide improved constraints on transit candidate size. We also find no evidence that narrowly separated KOI companions are more likely to be physically associated than widely separated companions, contrary to prior modeling work.

We have also reinterpreted 88 transit candidates, refining estimates of size given possible hosts and identifying 43 candidates potentially too large for planetary interpretation. With some assumptions, this produces an overall $P(R > 15R_{\oplus})$ for transits with detected contaminating companions of $17.5\%_{-3.7\%}^{+4.1\%}$, or an overall $P(R > 15R_{\oplus})$ for all KOIs (as a result of undetected companions) of $2.5\% \pm 0.4\%$. A more complete set of *JHK* follow-up on KOI companions would refine this result.

Given the termination of *Kepler*'s primary mission, solving host ambiguity for individual transit candidates is difficult. A close review of extant *Kepler* data for astrometric motion or light curve re-analysis may detect centroid motion correlated with transit that would identify the host star. Independent investigations like radial velocity and ground-based AO transit imaging are possible but difficult and limited to bright targets and deep transits, respectively.

ACKNOWLEDGMENTS

D.A. is supported by a NASA Space Technology Research Fellowship, grant NNX13AL75H. The authors thank the NSTRF staff and the Office of the Chief Technologist for their assistance. C.B. acknowledges support from the Alfred P. Sloan Foundation.

This work was partially supported by the NASA XRP grant NNX15AC91G.

The Robo-AO system was developed by collaborating partner institutions, the California Institute of Technol-

ogy and the Inter-University Centre for Astronomy and Astrophysics, and supported by the National Science Foundation under grants AST-0906060, AST-0960343, and AST-1207891, the Mt. Cuba Astronomical Foundation and by a gift from Samuel Oschin.

Some of the data presented herein were obtained at the W.M. Keck Observatory, which is operated as a scientific partnership among the California Institute of Technology, the University of California and the National Aeronautics and Space Administration. The Observatory was made possible by the generous financial support of the W.M. Keck Foundation.

The authors wish to recognize and acknowledge the very significant cultural role and reverence that the summit of Maunakea has always had within the indigenous Hawaiian community. We are most fortunate to have the opportunity to conduct observations from this mountain.

This paper includes data collected by the *Kepler* mission. Funding for the *Kepler* mission is provided by the NASA Science Mission directorate.

Some of the data presented in this paper were obtained from the Mikulski Archive for Space Telescopes (MAST). STScI is operated by the Association of Universities for Research in Astronomy, Inc., under NASA contract NAS5-26555. Support for MAST for non-HST data is provided by the NASA Office of Space Science via grant NNX09AF08G and by other grants and contracts.

Facilities: PO:1.5m (Robo-AO), Keck:II (NIRC2-LGS).

REFERENCES

- Adams, E. R., Ciardi, D. R., Dupree, A. K., Gautier, III, T. N., Kulesa, C., and McCarthy, D.: 2012, *AJ* **144**, 42
- Adams, E. R., Dupree, A. K., Kulesa, C., and McCarthy, D.: 2013, *AJ* **146**, 9
- Baranec, C., Riddle, R., Law, N. M., Ramaprakash, A. N., Tendulkar, S., Hogstrom, K., Bui, K., Burse, M., Chordia, P., Das, H., Dekany, R., Kulkarni, S., Punnadi, S., and Smith, R.: 2014, *ApJ* **790**, L8
- Baranec, C., Riddle, R., Law, N. M., Ramaprakash, A. N., Tendulkar, S. P., Bui, K., Burse, M. P., Chordia, P., Das, H. K., Davis, J. T. C., Dekany, R. G., Kasliwal, M. M., Kulkarni, S. R., Morton, T. D., Ofek, E. O., and Punnadi, S.: 2013, *Journal of Visualized Experiments* **72**, e50021
- Baranec, C., Ziegler, C., Law, N. M., Morton, T., Riddle, R., Atkinson, D., Schonhut, J., and Crepp, J.: 2016, *AJ* **152**, 18
- Batalha, N. M., Rowe, J. F., Gilliland, R. L., Jenkins, J. J., Caldwell, D., Borucki, W. J., Koch, D. G., Lissauer, J. J., Dunham, E. W., Gautier, T. N., Howell, S. B., Latham, D. W., Marcy, G. W., and Prsa, A.: 2010, *ApJ* **713**, L103
- Bechter, E. B., Crepp, J. R., Ngo, H., Knutson, H. A., Batygin, K., Hinkley, S., Muirhead, P. S., Johnson, J. A., Howard, A. W., Montet, B. T., Matthews, C. T., and Morton, T. D.: 2014, *ApJ* **788**, 2
- Becker, J. C., Vanderburg, A., Adams, F. C., Rappaport, S. A., and Schwengeler, H. M.: 2015, *ApJ* **812**, L18
- Borucki, W. J., Koch, D., Basri, G., Batalha, N., Brown, T., Caldwell, D., Caldwell, J., Christensen-Dalsgaard, J., Cochran, W. D., DeVore, E., Dunham, E. W., Dupree, A. K., Gautier, T. N., Geary, J. C., Gilliland, R., Gould, A., Howell, S. B., Jenkins, J. M., Kondo, Y., Latham, D. W., Marcy, G. W., Meibom, S., Kjeldsen, H., Lissauer, J. J., Monet, D. G., Morrison, D., Sasselov, D., Tarter, J., Boss, A., Brownlee, D., Owen, T., Buzasi, D., Charbonneau, D., Doyle, L., Fortney, J., Ford, E. B., Holman, M. J., Seager, S., Steffen, J. H., Welsh, W. F., Rowe, J., Anderson, H., Buchhave, L., Ciardi, D., Walkowicz, L., Sherry, W., Horch, E., Isaacson, H., Everett, M. E., Fischer, D., Torres, G., Johnson, J. A., Endl, M., MacQueen, P., Bryson, S. T., Dotson, J., Haas, M., Kolodziejczak, J., Van Cleve, J., Chandrasekaran, H., Twicken, J. D., Quintana, E. V., Clarke, B. D., Allen, C., Li, J., Wu, H., Tenenbaum, P., Verner, E., Bruhweiler, F., Barnes, J., and Prsa, A.: 2010, *Science* **327**, 977
- Brown, T. M.: 2003, *ApJ* **593**, L125
- Brown, T. M., Latham, D. W., Everett, M. E., and Esquerdo, G. A.: 2011, *AJ* **142**, 112
- Burgasser, A. J., Kirkpatrick, J. D., Reid, I. N., Brown, M. E., Miskey, C. L., and Gizis, J. E.: 2003, *ApJ* **586**, 512
- Cardelli, J. A., Clayton, G. C., and Mathis, J. S.: 1989, *ApJ* **345**, 245
- Ciardi, D. R., Beichman, C. A., Horch, E. P., and Howell, S. B.: 2015, *ApJ* **805**, 16
- Colón, K. D., Ford, E. B., and Morehead, R. C.: 2012, *MNRAS* **426**, 342
- Colón, K. D., Morehead, R. C., and Ford, E. B.: 2015, *MNRAS* **452**, 3001

- Coughlin, J. L., Mullally, F., Thompson, S. E., Rowe, J. F., Burke, C. J., Latham, D. W., Batalha, N. M., Ofir, A., Quarles, B. L., Henze, C. E., Wolfgang, A., Caldwell, D. A., Bryson, S. T., Shporer, A., Catanzarite, J., Akeson, R., Barclay, T., Borucki, W. J., Boyajian, T. S., Campbell, J. R., Christiansen, J. L., Girouard, F. R., Haas, M. R., Howell, S. B., Huber, D., Jenkins, J. M., Li, J., Patil-Sabale, A., Quintana, E. V., Ramirez, S., Seader, S., Smith, J. C., Tenenbaum, P., Twicken, J. D., and Zamudio, K. A.: 2015, *ArXiv e-prints*
- Coughlin, J. L., Thompson, S. E., Bryson, S. T., Burke, C. J., Caldwell, D. A., Christiansen, J. L., Haas, M. R., Howell, S. B., Jenkins, J. M., Kolodziejczak, J. J., Mullally, F. R., and Rowe, J. F.: 2014, *AJ* **147**, 119
- Désert, J.-M., Charbonneau, D., Torres, G., Fressin, F., Ballard, S., Bryson, S. T., Knutson, H. A., Batalha, N. M., Borucki, W. J., Brown, T. M., Deming, D., Ford, E. B., Fortney, J. J., Gilliland, R. L., Latham, D. W., and Seager, S.: 2015, *ApJ* **804**, 59
- Dressing, C. D., Adams, E. R., Dupree, A. K., Kulesa, C., and McCarthy, D.: 2014, *AJ* **148**, 78
- Fressin, F., Torres, G., Charbonneau, D., Bryson, S. T., Christiansen, J., Dressing, C. D., Jenkins, J. M., Walkowicz, L. M., and Batalha, N. M.: 2013, *ApJ* **766**, 81
- Habets, G. M. H. J. and Heintze, J. R. W.: 1981, *A&AS* **46**, 193
- Horch, E. P., Howell, S. B., Everett, M. E., and Ciardi, D. R.: 2012, *AJ* **144**, 165
- Horch, E. P., Howell, S. B., Everett, M. E., and Ciardi, D. R.: 2014, *ApJ* **795**, 60
- Huber, D., Silva Aguirre, V., Matthews, J. M., Pinsonneault, M. H., Gaidos, E., García, R. A., Hekker, S., Mathur, S., Mosser, B., Torres, G., Bastien, F. A., Basu, S., Bedding, T. R., Chaplin, W. J., Demory, B.-O., Fleming, S. W., Guo, Z., Mann, A. W., Rowe, J. F., Serenelli, A. M., Smith, M. A., and Stello, D.: 2014, *ApJS* **211**, 2
- Kraus, A. L. and Hillenbrand, L. A.: 2007, *AJ* **134**, 2340
- Law, N. M., Morton, T., Baranec, C., Riddle, R., Ravichandran, G., Ziegler, C., Johnson, J. A., Tendulkar, S. P., Bui, K., Burse, M. P., Das, H. K., Dekany, R. G., Kulkarni, S., Punnaadi, S., and Ramaprakash, A. N.: 2014, *ApJ* **791**, 35
- Liebert, J., Kirkpatrick, J. D., Beichman, C., Reid, I. N., Monet, D. G., and Dahn, C. C.: 1995, in *American Astronomical Society Meeting Abstracts*, Vol. 27 of *Bulletin of the American Astronomical Society*, p. 1391
- Lillo-Box, J., Barrado, D., and Bouy, H.: 2012, *A&A* **546**, A10
- Lillo-Box, J., Barrado, D., and Bouy, H.: 2014, *A&A* **566**, A103
- Mann, A. W., Gaidos, E., Lépine, S., and Hilton, E. J.: 2012, *ApJ* **753**, 90
- Morton, T. D.: 2012, *ApJ* **761**, 6
- Morton, T. D. and Johnson, J. A.: 2011, *ApJ* **738**, 170
- Muirhead, P. S., Hamren, K., Schlawin, E., Rojas-Ayala, B., Covey, K. R., and Lloyd, J. P.: 2012, *ApJ* **750**, L37
- Pecaut, M. J. and Mamajek, E. E.: 2013, *ApJS* **208**, 9
- Santerne, A., Fressin, F., Díaz, R. F., Figueira, P., Almenara, J.-M., and Santos, N. C.: 2013, *A&A* **557**, A139
- Schlafly, E. F. and Finkbeiner, D. P.: 2011, *ApJ* **737**, 103
- Service, M., Lu, J. R., Campbell, R., Sitarski, B. N., Ghez, A. M., and Anderson, J.: 2016, *PASP* In Press
- Slawson, R. W., Prša, A., Welsh, W. F., Orosz, J. A., Rucker, M., Batalha, N., Doyle, L. R., Engle, S. G., Conroy, K., Coughlin, J., Gregg, T. A., Fetherolf, T., Short, D. R., Windmiller, G., Fabrycky, D. C., Howell, S. B., Jenkins, J. M., Uddin, K., Mullally, F., Seader, S. E., Thompson, S. E., Sanderfer, D. T., Borucki, W., and Koch, D.: 2011, *AJ* **142**, 160
- STScI: 1997, *Mikulski Archive for Space Telescopes*, <http://archive.stsci.edu>
- Tenenbaum, P., Jenkins, J. M., Seader, S., Burke, C. J., Christiansen, J. L., Rowe, J. F., Caldwell, D. A., Clarke, B. D., Li, J., Quintana, E. V., Smith, J. C., Thompson, S. E., Twicken, J. D., Borucki, W. J., Batalha, N. M., Cote, M. T., Haas, M. R., Hunter, R. C., Sanderfer, D. T., Girouard, F. R., Hall, J. R., Ibrahim, K., Klaus, T. C., McCauliff, S. D., Middour, C. K., Sabale, A., Uddin, A. K., Wohler, B., Barclay, T., and Still, M.: 2013, *ApJS* **206**, 5
- van Dam, M. A., Bouchez, A. H., Le Mignant, D., Johansson, E. M., Wizinowich, P. L., Campbell, R. D., Chin, J. C. Y., Hartman, S. K., Lafon, R. E., Stomski, Jr., P. J., and Summers, D. M.: 2006, *PASP* **118**, 310
- Wang, J., Fischer, D. A., Horch, E. P., and Xie, J.-W.: 2015, *ApJ* **806**, 248
- Wang, J., Xie, J.-W., Barclay, T., and Fischer, D. A.: 2014, *ApJ* **783**, 4
- Wizinowich, P. L., Le Mignant, D., Bouchez, A. H., Campbell, R. D., Chin, J. C. Y., Contos, A. R., van Dam, M. A., Hartman, S. K., Johansson, E. M., Lafon, R. E., Lewis, H., Stomski, P. J., Summers, D. M., Brown, C. G., Danforth, P. M., Max, C. E., and Pennington, D. M.: 2006, *PASP* **118**, 297
- Yelda, S., Lu, J. R., Ghez, A. M., Clarkson, W., Anderson, J., Do, T., and Matthews, K.: 2010, *ApJ* **725**, 331
- Ziegler, C., Law, N. M., Morton, T., Baranec, C., Riddle, R., Atkinson, D., Baker, A., Roberts, S., and Ciardi, D. R.: 2016, *ArXiv e-prints*

TABLE 4 Measured *JHK* Contrasts

object	sep(")	ang(°)	Δm_J (mag)	Δm_H (mag)	Δm_K (mag)
0190B	0.180 ± 0.010	109.4 ± 3.2			0.642 ± 0.137
0191B	1.660 ± 0.002	96.6 ± 0.1	2.588 ± 0.057	2.615 ± 0.054	2.626 ± 0.055
0268B	1.753 ± 0.003	267.6 ± 0.1	3.056 ± 0.059	2.654 ± 0.057	2.553 ± 0.056
0268C	2.528 ± 0.007	310.2 ± 0.1	3.810 ± 0.118	3.353 ± 0.127	3.984 ± 0.145
0401B	1.986 ± 0.002	270.0 ± 0.1	2.066 ± 0.059		1.635 ± 0.055
0425B	0.491 ± 0.001	343.4 ± 0.1			0.831 ± 0.054
0511B	1.300 ± 0.002	123.4 ± 0.1	2.221 ± 0.058	1.817 ± 0.007	1.707 ± 0.008
0511C	3.865 ± 0.005	348.6 ± 0.1	5.055 ± 0.122	4.493 ± 0.077	4.308 ± 0.069
0628B	2.748 ± 0.002	238.9 ± 0.1			3.000 ± 0.058
0628C	1.828 ± 0.003	311.5 ± 0.2			3.871 ± 0.057
0687B	0.680 ± 0.003	13.4 ± 0.4			1.251 ± 0.054
0688B	1.734 ± 0.001	141.8 ± 0.1	1.552 ± 0.060		1.373 ± 0.056
0712B	0.470 ± 0.002	174.2 ± 0.3	0.435 ± 0.055		0.351 ± 0.056
0931B	1.263 ± 0.002	177.7 ± 0.1			3.227 ± 0.063
0984B	1.764 ± 0.005	221.3 ± 1.4	0.064 ± 0.058	0.050 ± 0.054	0.059 ± 0.056
0987B	1.974 ± 0.002	225.7 ± 0.3	2.612 ± 0.077	2.381 ± 0.058	2.239 ± 0.055
1066B	1.690 ± 0.002	231.3 ± 0.1			2.949 ± 0.070
1067B	2.932 ± 0.005	142.6 ± 0.1			2.785 ± 0.106
1112B	3.068 ± 0.005	172.2 ± 0.1	3.607 ± 0.138	2.956 ± 0.081	2.758 ± 0.070
1151B	0.758 ± 0.002	307.5 ± 0.7		2.554 ± 0.055	2.407 ± 0.055
1214B	0.371 ± 0.029	136.3 ± 0.3		2.584 ± 0.055	2.455 ± 0.055
1274B	1.085 ± 0.001	242.0 ± 0.1	2.801 ± 0.056		2.506 ± 0.055
1359B	1.387 ± 0.003	331.6 ± 0.4			2.168 ± 0.057
1375B	0.784 ± 0.001	270.0 ± 0.1		3.303 ± 0.069	3.393 ± 0.065
1442B	2.114 ± 0.006	70.8 ± 0.1	4.155 ± 0.065	3.802 ± 0.056	3.631 ± 0.055
1447B	0.282 ± 0.001	212.0 ± 0.1			0.625 ± 0.061

object	sep('')	ang(°)	Δm_J (mag)	Δm_H (mag)	Δm_K (mag)
1536B	0.580 ± 0.001	97.9 ± 0.1		4.262 ± 0.136	4.177 ± 0.112
1546B	0.603 ± 0.002	89.5 ± 0.1	0.940 ± 0.055	0.784 ± 0.055	0.726 ± 0.054
1546C	2.915 ± 0.001	4.0 ± 0.1	3.224 ± 0.059	3.021 ± 0.071	2.945 ± 0.081
1546D	4.119 ± 0.011	164.7 ± 0.1	3.338 ± 0.073	3.253 ± 0.077	3.479 ± 0.058
1613B	0.214 ± 0.004	185.5 ± 1.3	1.136 ± 0.055	0.996 ± 0.055	0.997 ± 0.055
1700B	0.274 ± 0.048	288.1 ± 10.7			0.551 ± 0.055
1784B	0.278 ± 0.001	291.1 ± 0.1			0.781 ± 0.058
1845B	1.999 ± 0.011	78.9 ± 0.5	3.238 ± 0.055		2.886 ± 0.055
1845C	2.958 ± 0.025	348.0 ± 0.2	4.264 ± 0.069		4.400 ± 0.092
1880B	1.713 ± 0.001	100.9 ± 0.1	3.936 ± 0.058	4.149 ± 0.057	4.282 ± 0.058
1884B	0.934 ± 0.001	95.6 ± 0.1	2.642 ± 0.056	2.410 ± 0.056	2.305 ± 0.055
1884C	1.838 ± 0.001	81.9 ± 0.1	3.075 ± 0.056	2.867 ± 0.057	2.731 ± 0.055
1884D	2.567 ± 0.002	327.5 ± 0.1	3.590 ± 0.164	3.536 ± 0.141	3.204 ± 0.141
1891B	2.066 ± 0.003	211.4 ± 0.1	4.340 ± 0.077	4.561 ± 0.060	4.596 ± 0.066
1916B	0.252 ± 0.001	146.3 ± 0.1	1.201 ± 0.056		1.054 ± 0.055
1979B	0.842 ± 0.002	193.4 ± 0.1	2.291 ± 0.055		1.822 ± 0.055
1989B	0.816 ± 0.001	39.5 ± 0.1			2.921 ± 0.055
2001B	1.167 ± 0.001	342.0 ± 0.1			4.320 ± 0.060
2009B	1.513 ± 0.004	178.0 ± 0.1	3.042 ± 0.092	2.950 ± 0.061	2.750 ± 0.055
2059B	0.394 ± 0.001	290.0 ± 0.1			0.539 ± 0.151
2069B	1.128 ± 0.001	107.0 ± 0.1			3.195 ± 0.059
2083B	0.255 ± 0.002	166.1 ± 0.3		1.687 ± 0.056	1.600 ± 0.054
2117B	0.334 ± 0.001	111.5 ± 0.1			0.531 ± 0.055
2143B	2.184 ± 0.005	317.4 ± 0.1	3.200 ± 0.120		3.457 ± 0.087
2159B	2.009 ± 0.001	323.8 ± 0.1		2.638 ± 0.063	2.476 ± 0.060
2247B	1.917 ± 0.002	350.3 ± 0.1			3.867 ± 0.068
2289B	0.948 ± 0.001	221.7 ± 0.1			2.938 ± 0.055
2317B	1.512 ± 0.002	112.2 ± 0.1			3.923 ± 0.058
2363B	1.952 ± 0.001	357.3 ± 0.1			5.041 ± 0.086
2377B	2.185 ± 0.002	335.2 ± 0.1	0.828 ± 0.080	0.671 ± 0.073	0.629 ± 0.068
2377C	3.903 ± 0.008	315.9 ± 0.1	3.925 ± 0.193	3.816 ± 0.146	3.551 ± 0.170
2377D	2.540 ± 0.002	41.5 ± 0.1	4.234 ± 0.096	4.029 ± 0.116	3.752 ± 0.117
2413B	0.308 ± 0.036	250.1 ± 8.7		0.470 ± 0.109	0.170 ± 0.059
2443B	1.384 ± 0.002	164.0 ± 0.1	4.133 ± 0.066		3.632 ± 0.060
2542B	0.769 ± 0.002	29.1 ± 0.2	0.896 ± 0.055		0.602 ± 0.054
2554B	0.372 ± 0.010	149.3 ± 1.6			0.267 ± 0.054
2554C	3.547 ± 0.005	203.6 ± 0.1			2.960 ± 0.098
2601B	1.598 ± 0.002	14.1 ± 0.1			0.966 ± 0.057
2601C	1.480 ± 0.002	295.2 ± 0.1			2.979 ± 0.057
2601D	3.059 ± 0.003	30.1 ± 0.2			4.899 ± 0.135
2657B	0.744 ± 0.365	131.7 ± 1.8	0.145 ± 0.055	0.126 ± 0.055	0.106 ± 0.054
2664B	1.190 ± 0.005	90.5 ± 0.2			1.103 ± 0.055
2681B	1.132 ± 0.005	148.0 ± 0.3			0.431 ± 0.056
2705B	1.900 ± 0.003	304.3 ± 0.2	2.565 ± 0.097	2.672 ± 0.099	2.584 ± 0.067
2711B	0.472 ± 0.006	148.9 ± 0.2	0.149 ± 0.055	0.122 ± 0.055	0.118 ± 0.055
2722B	3.224 ± 0.001	283.3 ± 0.2		3.937 ± 0.084	3.770 ± 0.064
2779B	0.965 ± 0.010	66.5 ± 0.6			1.752 ± 0.055
2813B	1.062 ± 0.001	261.1 ± 0.1			1.842 ± 0.055
2813C	1.842 ± 0.005	187.8 ± 0.2			6.547 ± 0.237
2837B	0.355 ± 0.018	140.5 ± 2.8	0.218 ± 0.056	0.199 ± 0.055	0.200 ± 0.055
2859B	0.454 ± 0.001	290.9 ± 0.1	3.262 ± 0.067	3.138 ± 0.066	2.890 ± 0.059
2869B	1.625 ± 0.001	205.2 ± 0.1			5.670 ± 0.074
2904B	0.699 ± 0.001	225.6 ± 0.1	2.705 ± 0.055	2.501 ± 0.055	2.446 ± 0.054
2971B	0.300 ± 0.001	273.9 ± 0.1	4.503 ± 0.130		3.568 ± 0.057
2971C	3.561 ± 0.004	37.7 ± 0.1	7.656 ± 0.219		5.931 ± 0.170
3020B	0.379 ± 0.001	271.6 ± 0.1			1.266 ± 0.057
3020C	3.862 ± 0.001	231.3 ± 0.1			5.008 ± 0.069
3029B	0.251 ± 0.010	264.3 ± 2.3			0.135 ± 0.060
3029C	2.543 ± 0.005	4.1 ± 0.1			3.440 ± 0.068
3029D	1.734 ± 0.005	356.2 ± 0.2			4.489 ± 0.071
3069B	1.790 ± 0.002	108.3 ± 0.1	1.579 ± 0.056	1.310 ± 0.055	1.265 ± 0.056
3106B	0.272 ± 0.010	186.3 ± 2.2			1.221 ± 0.131
3377B	0.265 ± 0.001	334.7 ± 0.1			0.485 ± 0.058
3377C	1.406 ± 0.005	50.2 ± 0.2			3.741 ± 0.063
3401B	0.648 ± 0.010	98.9 ± 0.9			1.877 ± 0.057
4004B	1.954 ± 0.003	218.1 ± 0.1			2.373 ± 0.076
4209B	0.976 ± 0.001	205.1 ± 0.1	0.322 ± 0.059	0.539 ± 0.056	0.570 ± 0.055
4292B	1.950 ± 0.002	29.9 ± 0.1		4.813 ± 0.075	4.542 ± 0.079
4331B	0.335 ± 0.005	100.9 ± 1.0		0.118 ± 0.055	0.125 ± 0.054
4407B	2.453 ± 0.003	299.9 ± 0.1	2.286 ± 0.056	1.956 ± 0.056	1.893 ± 0.058
4407C	2.660 ± 0.003	311.0 ± 0.1	4.479 ± 0.490	4.140 ± 0.712	4.654 ± 0.344
4463B	2.457 ± 0.003	323.9 ± 0.1	0.160 ± 0.102	0.242 ± 0.082	0.259 ± 0.068
4634B	0.281 ± 0.001	276.1 ± 0.1			0.653 ± 0.055
4768B	1.339 ± 0.005	159.0 ± 0.2			2.608 ± 0.071
4822B	0.559 ± 0.010	63.2 ± 1.0			4.503 ± 0.147
4871B	0.922 ± 0.001	333.6 ± 0.1	3.126 ± 0.058	3.026 ± 0.057	3.038 ± 0.055
5578B	0.322 ± 0.001	97.2 ± 0.1			1.681 ± 0.055
5762B	0.221 ± 0.010	100.3 ± 2.5			0.833 ± 0.076

TABLE 4 Relative locations and NIR contrast measurements of observed *Kepler* Objects of Interest. Contrast uncertainties are systematically measured by varying the photometric aperture size. Use of co-added images reduces separation/angle measurement uncertainties to the single-pixel level.

TABLE 5 Apparent Magnitudes of Resolved KOI Components

object	sep('')	ang(°)	Δm_J (mag)	Δm_H (mag)	Δm_K (mag)
KOI	m_J	m_H	m_K	m_i	m_{Kep}
0190A			12.876 \pm 0.053		14.419 \pm 0.050
0190B			13.517 \pm 0.089		15.748 \pm 0.137
0191A	13.827 \pm 0.023	13.419 \pm 0.026	13.340 \pm 0.037		15.057 \pm 0.042
0191B	16.414 \pm 0.057	16.032 \pm 0.056	15.961 \pm 0.062		18.156 \pm 0.453
0268A	9.773 \pm 0.021	9.609 \pm 0.023	9.518 \pm 0.019		10.599 \pm 0.301
0268B	12.826 \pm 0.059	12.259 \pm 0.056	12.074 \pm 0.056		14.603 \pm 0.317
0268C	13.573 \pm 0.117	12.963 \pm 0.123	13.499 \pm 0.144		16.199 \pm 0.314
0401A	12.845 \pm 0.023		12.402 \pm 0.027		14.076 \pm 0.036
0401B	14.909 \pm 0.056		14.037 \pm 0.051		16.975 \pm 0.261
0425A			13.571 \pm 0.043		15.101 \pm 0.043
0425B			14.401 \pm 0.056		15.957 \pm 0.076
0511A	13.222 \pm 0.023	12.957 \pm 0.035	12.883 \pm 0.034		14.276 \pm 0.036
0511B	15.444 \pm 0.059	14.816 \pm 0.056	14.647 \pm 0.055		17.387 \pm 0.355
0511C	18.280 \pm 0.127	17.449 \pm 0.084	17.194 \pm 0.077		20.649 \pm 0.383
0628A			12.484 \pm 0.025	13.773 \pm 0.020	
0628B			15.486 \pm 0.061	18.287 \pm 0.138	
0628C			16.356 \pm 0.059	18.591 \pm 0.217	
0687A			12.415 \pm 0.026	13.771 \pm 0.042	
0687B			13.667 \pm 0.046	15.808 \pm 0.238	
0688A	13.158 \pm 0.028		12.858 \pm 0.023		14.129 \pm 0.044
0688B	14.708 \pm 0.054		14.231 \pm 0.049		16.316 \pm 0.244
0712A	13.176 \pm 0.032		12.771 \pm 0.030	13.831 \pm 0.072	
0712B	13.615 \pm 0.040		13.123 \pm 0.037	15.010 \pm 0.207	
0931A			13.828 \pm 0.049		15.318 \pm 0.030
0931B			17.055 \pm 0.079		18.719 \pm 0.136
0984A	11.178 \pm 0.037	10.823 \pm 0.036	10.741 \pm 0.034	12.100 \pm 0.072	12.340 \pm 0.049
0984B	11.242 \pm 0.036	10.873 \pm 0.036	10.797 \pm 0.036	12.113 \pm 0.074	12.430 \pm 0.049
0987A	11.328 \pm 0.021	10.951 \pm 0.020	10.906 \pm 0.013	12.356 \pm 0.027	12.590 \pm 0.030
0987B	13.940 \pm 0.074	13.331 \pm 0.055	13.146 \pm 0.050	16.423 \pm 0.629	16.158 \pm 0.103
1066A			13.922 \pm 0.040		15.647 \pm 0.030
1066B			16.950 \pm 0.077		19.837 \pm 0.184
1067A			13.313 \pm 0.035		14.710 \pm 0.029
1067B			16.095 \pm 0.105		18.762 \pm 0.157
1112A	13.509 \pm 0.050	13.251 \pm 0.039	13.155 \pm 0.049		14.650 \pm 0.029
1112B	17.122 \pm 0.146	16.204 \pm 0.085	15.913 \pm 0.081		19.222 \pm 0.057
1151A		11.917 \pm 0.020	11.857 \pm 0.021	13.249 \pm 0.035	
1151B		14.474 \pm 0.053	14.263 \pm 0.054	16.716 \pm 0.562	
1214A		13.092 \pm 0.027	12.978 \pm 0.028		14.933 \pm 0.051
1214B		15.678 \pm 0.054	15.431 \pm 0.054		16.139 \pm 0.134
1274A	12.088 \pm 0.020		11.638 \pm 0.017	13.142 \pm 0.025	
1274B	14.892 \pm 0.055		14.143 \pm 0.052	16.911 \pm 0.429	
1375A		12.310 \pm 0.020	12.279 \pm 0.018	13.554 \pm 0.022	
1375B		15.613 \pm 0.070	15.668 \pm 0.064	17.936 \pm 0.506	
1442A	11.354 \pm 0.024	11.015 \pm 0.028	10.947 \pm 0.022	12.298 \pm 0.020	
1442B	15.507 \pm 0.067	14.819 \pm 0.060	14.581 \pm 0.058	18.971 \pm 0.563	
1447A			12.292 \pm 0.030		13.248 \pm 0.039
1447B			12.917 \pm 0.043		15.288 \pm 0.160
1536A		11.405 \pm 0.017	11.349 \pm 0.018	12.550 \pm 0.020	
1536B		15.669 \pm 0.135	15.532 \pm 0.114	17.816 \pm 0.570	
1546A	13.783 \pm 0.030	13.459 \pm 0.029	13.373 \pm 0.030		14.760 \pm 0.095
1546B	14.725 \pm 0.047	14.245 \pm 0.045	14.096 \pm 0.045		16.318 \pm 0.377
1546C	17.121 \pm 0.077	16.711 \pm 0.079	16.851 \pm 0.062		18.587 \pm 0.530
1546D	17.010 \pm 0.064	16.479 \pm 0.072	16.319 \pm 0.085		18.615 \pm 0.560
1613A	10.915 \pm 0.025	10.680 \pm 0.027	10.647 \pm 0.024	†	
1613B	12.049 \pm 0.046	11.677 \pm 0.048	11.643 \pm 0.043	†	
1700A			12.890 \pm 0.030		14.822 \pm 0.079
1700B			13.446 \pm 0.040		15.893 \pm 0.192
1784A			12.533 \pm 0.027		14.093 \pm 0.055
1784B			13.310 \pm 0.043		14.674 \pm 0.087
1845A	12.881 \pm 0.023		12.281 \pm 0.021	*	*
1845B	16.119 \pm 0.057		15.166 \pm 0.053	*	*
1845C	17.146 \pm 0.071		16.680 \pm 0.092	*	*
1880A	12.293 \pm 0.022	11.634 \pm 0.018	11.474 \pm 0.012		14.480 \pm 0.033
1880B	16.231 \pm 0.059	15.785 \pm 0.059	15.754 \pm 0.058		18.146 \pm 0.441
1884A	14.196 \pm 0.045	13.789 \pm 0.057	13.738 \pm 0.060		15.509 \pm 0.035
1884B	16.836 \pm 0.067	16.200 \pm 0.079	16.041 \pm 0.078		19.617 \pm 0.588
1884C	17.268 \pm 0.068	16.652 \pm 0.079	16.468 \pm 0.079		20.383 \pm 0.436
1884D	17.794 \pm 0.165	17.321 \pm 0.144	16.943 \pm 0.146		21.075 \pm 0.349
1891A	13.879 \pm 0.021	13.331 \pm 0.028	13.274 \pm 0.029		15.284 \pm 0.031

KOI	m_J	m_H	m_K	m_i	m_{Kep}
1891B	18.220 \pm 0.077	17.895 \pm 0.062	17.872 \pm 0.068		19.545 \pm 0.444
1916A	12.797 \pm 0.023		12.493 \pm 0.026		13.684 \pm 0.035
1916B	14.002 \pm 0.047		13.547 \pm 0.046		16.421 \pm 0.229
1979A	11.941 \pm 0.025		11.601 \pm 0.014	12.845 \pm 0.029	
1979B	14.235 \pm 0.057		13.423 \pm 0.045	16.047 \pm 0.366	
1989A			11.841 \pm 0.018	13.144 \pm 0.024	13.372 \pm 0.030
1989B			14.766 \pm 0.054	17.363 \pm 0.535	16.866 \pm 0.151
2001A			11.144 \pm 0.019	12.835 \pm 0.020	13.135 \pm 0.030
2001B			15.463 \pm 0.060	17.411 \pm 0.258	17.617 \pm 0.219
2009A	12.714 \pm 0.021	12.387 \pm 0.021	12.333 \pm 0.022		13.848 \pm 0.033
2009B	15.751 \pm 0.089	15.335 \pm 0.061	15.085 \pm 0.055		17.929 \pm 0.491
2059A			11.182 \pm 0.063		13.246 \pm 0.048
2059B			11.724 \pm 0.098		14.339 \pm 0.104
2069A			12.231 \pm 0.020	13.582 \pm 0.020	13.777 \pm 0.031
2069B			15.422 \pm 0.060	18.874 \pm 0.508	18.026 \pm 0.504
2083A		12.263 \pm 0.020	12.230 \pm 0.024	13.446 \pm 0.037	13.871 \pm 0.056
2083B		13.948 \pm 0.050	13.827 \pm 0.050	16.164 \pm 0.359	14.907 \pm 0.134
2117A			13.516 \pm 0.037		16.236 \pm 0.032
2117B			14.047 \pm 0.046		16.567 \pm 0.034
2143A	12.924 \pm 0.025		12.505 \pm 0.026		14.145 \pm 0.031
2143B	16.122 \pm 0.118		15.965 \pm 0.088		17.654 \pm 0.283
2159A		12.098 \pm 0.019	12.087 \pm 0.021	13.322 \pm 0.025	
2159B		14.731 \pm 0.058	14.563 \pm 0.059	17.340 \pm 0.512	
2247A			12.046 \pm 0.022		14.384 \pm 0.029
2247B			15.916 \pm 0.069		19.508 \pm 0.213
2289A			12.075 \pm 0.018	13.214 \pm 0.021	13.374 \pm 0.030
2289B			15.012 \pm 0.055	17.540 \pm 0.285	18.008 \pm 0.297
2317A			12.704 \pm 0.026		14.298 \pm 0.031
2317B			16.628 \pm 0.063		19.227 \pm 0.194
2363A			12.360 \pm 0.018		14.369 \pm 0.031
2363B			17.407 \pm 0.085		20.945 \pm 1.338
2377A	13.673 \pm 0.038	13.286 \pm 0.045	13.245 \pm 0.040	*	*
2377B	14.501 \pm 0.063	13.958 \pm 0.062	13.876 \pm 0.057	*	*
2377C	17.598 \pm 0.196	17.112 \pm 0.148	16.785 \pm 0.173	*	*
2377D	17.909 \pm 0.105	17.318 \pm 0.126	17.004 \pm 0.120	*	*
2413A		13.352 \pm 0.046	13.345 \pm 0.041		15.236 \pm 0.101
2413B		13.820 \pm 0.068	13.515 \pm 0.044		17.342 \pm 0.554
2443A	12.933 \pm 0.024		12.574 \pm 0.022		13.995 \pm 0.030
2443B	17.070 \pm 0.070		16.209 \pm 0.063		19.395 \pm 0.540
2542A	13.253 \pm 0.027		12.525 \pm 0.034		15.841 \pm 0.056
2542B	14.147 \pm 0.043		13.125 \pm 0.043		17.037 \pm 0.142
2554A			13.708 \pm 0.042	*	*
2554B			13.977 \pm 0.049	*	*
2554C			16.667 \pm 0.101	*	*
2601A			12.850 \pm 0.032		14.222 \pm 0.111
2601B			13.816 \pm 0.051		15.646 \pm 0.384
2601C			15.828 \pm 0.065		18.129 \pm 0.245
2601D			17.752 \pm 0.137		19.872 \pm 1.153
2657A	12.333 \pm 0.032	11.978 \pm 0.031	11.936 \pm 0.031		13.497 \pm 0.084
2657B	12.477 \pm 0.035	12.104 \pm 0.033	12.041 \pm 0.033		13.770 \pm 0.103
2664A			13.877 \pm 0.041		16.065 \pm 0.040
2664B			14.979 \pm 0.056		16.897 \pm 0.065
2681A			14.460 \pm 0.057		16.295 \pm 0.040
2681B			14.890 \pm 0.063		17.547 \pm 0.091
2705A	11.667 \pm 0.025	11.016 \pm 0.028	10.822 \pm 0.024		14.765 \pm 0.297
2705B	14.232 \pm 0.091	13.690 \pm 0.094	13.404 \pm 0.064		17.956 \pm 0.328
2711A	13.248 \pm 0.033	12.982 \pm 0.033	12.992 \pm 0.033		14.337 \pm 0.046
2711B	13.397 \pm 0.038	13.103 \pm 0.035	13.111 \pm 0.038		14.457 \pm 0.052
2722A		12.110 \pm 0.023	12.026 \pm 0.018		13.274 \pm 0.029
2722B		16.049 \pm 0.082	15.795 \pm 0.067		19.149 \pm 0.138
2779A			13.623 \pm 0.039		15.040 \pm 0.048
2779B			15.376 \pm 0.060		17.586 \pm 0.332
2813A			11.697 \pm 0.020		13.951 \pm 0.068
2813B			13.540 \pm 0.050		14.958 \pm 0.155
2813C			18.263 \pm 0.244		22.013 \pm 0.680
2837A	12.997 \pm 0.033	12.822 \pm 0.031	12.800 \pm 0.032		13.873 \pm 0.035
2837B	13.212 \pm 0.036	13.022 \pm 0.035	13.000 \pm 0.036		14.102 \pm 0.037
2859A	12.589 \pm 0.021	12.181 \pm 0.016	12.125 \pm 0.016		13.997 \pm 0.044
2859B	15.849 \pm 0.067	15.323 \pm 0.066	15.013 \pm 0.056		16.118 \pm 0.215
2869A			12.367 \pm 0.018		13.750 \pm 0.029
2869B			18.039 \pm 0.074		21.629 \pm 0.163
2904A	11.766 \pm 0.021	11.518 \pm 0.022	11.467 \pm 0.018		12.848 \pm 0.045
2904B	14.474 \pm 0.053	14.017 \pm 0.054	13.911 \pm 0.051		14.833 \pm 0.206
2971A	11.792 \pm 0.021		11.482 \pm 0.016		12.769 \pm 0.031
2971B	16.289 \pm 0.126		15.053 \pm 0.056		16.840 \pm 0.094
2971C	19.444 \pm 0.225		17.411 \pm 0.167		20.654 \pm 1.884
3020A			12.323 \pm 0.023		13.591 \pm 0.031
3020B			13.586 \pm 0.046		16.818 \pm 0.104
3020C			17.328 \pm 0.072		20.511 \pm 0.335

KOI	m_J	m_H	m_K	m_i	m_{Kep}
3029A			13.869 \pm 0.040	*	*
3029B			14.004 \pm 0.043	*	*
3029C			17.309 \pm 0.076	*	*
3029D			18.358 \pm 0.083	*	*
3069A	13.916 \pm 0.033	13.561 \pm 0.032	13.482 \pm 0.037		15.049 \pm 0.032
3069B	15.496 \pm 0.054	14.872 \pm 0.052	14.747 \pm 0.054		17.249 \pm 0.065
3106A			14.018 \pm 0.052		15.858 \pm 0.060
3106B			15.233 \pm 0.108		16.605 \pm 0.111
3377A			13.321 \pm 0.034		15.355 \pm 0.029
3377B			13.805 \pm 0.043		19.175 \pm 0.190
3377C			17.062 \pm 0.070		21.181 \pm 0.284
3401A			12.909 \pm 0.026		14.788 \pm 0.069
3401B			14.782 \pm 0.054		15.679 \pm 0.144
4004A			11.221 \pm 0.021		12.722 \pm 0.031
4004B			13.596 \pm 0.069		16.732 \pm 0.111
4209A	15.098 \pm 0.042	14.635 \pm 0.060	14.496 \pm 0.056		16.073 \pm 0.095
4209B	15.421 \pm 0.047	15.172 \pm 0.066	15.066 \pm 0.063		18.759 \pm 0.758
4292A		11.340 \pm 0.017	11.294 \pm 0.011		12.897 \pm 0.030
4292B		16.152 \pm 0.076	15.837 \pm 0.075		20.932 \pm 0.343
4331A		12.697 \pm 0.033	12.629 \pm 0.032		13.869 \pm 0.296
4331B		12.816 \pm 0.037	12.755 \pm 0.035		14.118 \pm 0.296
4407A	10.292 \pm 0.026	10.071 \pm 0.029	9.9666 \pm 0.018	*	*
4407B	12.579 \pm 0.055	12.029 \pm 0.057	11.859 \pm 0.053	*	*
4407C	14.782 \pm 0.475	14.180 \pm 0.695	14.610 \pm 0.341	*	*
4463A	13.575 \pm 0.054	13.189 \pm 0.046	13.175 \pm 0.043		16.347 \pm 0.033
4463B	13.728 \pm 0.059	13.428 \pm 0.052	13.435 \pm 0.048		16.356 \pm 0.033
4634A			12.725 \pm 0.031		13.876 \pm 0.080
4634B			13.380 \pm 0.042		15.753 \pm 0.386
4768A			13.886 \pm 0.050		15.738 \pm 0.029
4768B			16.495 \pm 0.265		19.726 \pm 0.260
4822A			12.062 \pm 0.016		13.475 \pm 0.030
4822B			16.573 \pm 0.144		20.183 \pm 0.443
4871A	12.125 \pm 0.023	11.884 \pm 0.022	11.843 \pm 0.013		13.107 \pm 0.032
4871B	15.254 \pm 0.060	14.908 \pm 0.058	14.880 \pm 0.054		16.225 \pm 0.189
5578A			9.7288 \pm 0.018		11.281 \pm 0.048
5578B			11.410 \pm 0.047		13.057 \pm 0.193
5762A			14.158 \pm 0.056		16.115 \pm 0.097
5762B			14.993 \pm 0.073		16.764 \pm 0.169

TABLE 5 Apparent magnitudes of individual stars from contrast measurements and literature values of blended system. The great majority of JHK values are from the 2MASS catalog (Liebert et al. 1995), while sources for i and *Kepler* are more varied. All values are as reported in the Exoplanet Archive, except *JHK* for KOI0268, which is linked to a spurious 2MASS entry. * indicates that not all companions were detected by Robo-AO. Without contrast measurements for all objects we can not accurately determine the apparent magnitudes. † indicates that although a contrast measurement has been made, there is no blended measurement, and we can not determine the apparent magnitude.